C.P. No. 911

C.P. No. 911

MINISTRY OF AVIATION

AERONAUTICAL RESEARCH COUNCIL

CURRENT PAPERS

Studies of Flow Fields Created by Vertical and Inclined Jets when Stationary or Moving over a Horizontal Surface

By

W. A. Abbott

LONDON: HER MAJESTY'S STATIONERY OFFICE

1967

EIGHT SHILLINGS NET

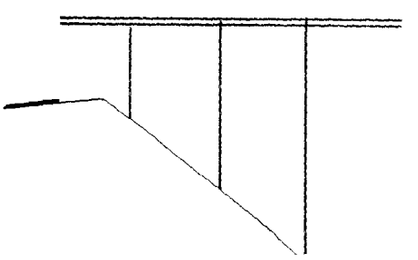

U.D.C. No. 532.525.533.691.18

C.P. No. 911*

October, 1964

Studies of flow fields created by vertical and inclined jets when stationary or moving over a horizontal surface

- by -

W. A. Abbott

SUMMARY

Model tests have been carried out with single and twin nozzle arrangements, at varying inclinations. The decay of maximum velocity and temperature of the jet after impingement on the ground has been measured.

Transient effects associated with swivelling nozzles have been studied and measurements of the upwind extent and height of the exhaust cloud were made with the nozzles moving over the ground (taxiing). Empirical rules are given for estimating these effects from measurements made under static, steady-flow conditions.

*Replaces N.G.T.E. M.391 - A.R.C. 26 624

CONTENTS

APPENDICES

ILLUSTRATIONS

ILLUSTRATIONS (cont'd)

1.0 Introduction

With certain V.T.O.L. aircraft configurations it may be possible to eliminate re-ingestion of exhaust gases into the engine intakes by employing a "rolling take-off" so that the exhaust gases are blown clear of the intakes by the relative wind.

Model tests have been carried out in which several nozzle arrangements have been made to traverse the ground with constant velocity. The upwind extent of the flow from these nozzles has been measured and an attempt has been made to correlate these readings with the steady state decay of dynamic head of the jets from the respective stationary nozzle arrangement.

The growth of the exhaust cloud on swivelling the nozzle system from a horizontal direction into the vertical position was also studied for the stationary and moving nozzle arrangements and an attempt was also made to correlate these results with the respective steady state readings.

2.0 Steady state tests

2.1 Decay of maximum dynamic head after jet impingement

The nozzles which were used in the tests are shown in Figure 1; a full scale nozzle of about 20 in. diameter was represented at either $\frac{1}{10}$ or $\frac{1}{20}$ scale.

Measurements of the maximum dynamic head of the jet after impingement were made using a pitot tube of 1 mm diameter connected to a sensitive micromanometer. The maximum dynamic head reading at any radial point was obtained by traversing the pitot tube in a vertical direction from the ground; the maximum reading occurred at heights of less than an inch. The jet exit total head was also measured.

Initial tests were carried out with the single 2 in. diameter conical nozzle (Figure 1b) mounted vertically with the exit 2 in. above the ground and total head measurements were made near the ground along a radius from the point of jet impingement as in Reference 1. Results with cold air for a range of jet total pressures from 1.6 to 18 in.Hg are plotted in Figure 2. It can be seen that by plotting the results in the form of $\left(\frac{q}{q_J}\right)^{\frac{1}{2}}$ they are independent of jet dynamic head, q_J.

In order to investigate the effect of nozzle discharge coefficient a 2 in. diameter orifice was tested in the same manner as the nozzle above and the results are plotted on Figure 2.

The discharge coefficients of the 2 in. conical nozzle and the 2 in. orifice were measured using a calibrated orifice-plate meter and are shown in Figure 2. The variation of discharge coefficient with jet pressure is in accord with Reference 2. It can be seen that if the values of $\left(\frac{q}{q_J}\right)^{\frac{1}{2}}$ were replotted versus $\frac{R}{\sqrt{C_D}\, D_J}$ instead of R/D_J they would be coincident for the nozzle and the orifice. This suggests that $\sqrt{C_D} \cdot D_J$ might

be the pertinent parameter with which to form the non-dimensional distance. However, as all later tests were carried out with the convergent type of nozzles (Figure 1) the distances have been presented in the simpler form R/D_J.

A series of tests with inclined nozzles was carried out in which the total head measurements were made near the ground in the plane of inclination of the nozzles. Total head measurements were made both in front of and behind the jet and are plotted in Figure 4. (See Figure 3 for nomenclature.) In all cases the nozzle slant height S was less than 6 D_J. The three points for tests with heated air confirm that, as with the vertical jet[1], $\left(\frac{q}{q_J}\right)^{\frac{1}{2}}$ at any point is independent of θ_J as well as of q_J.

Straight line characteristics of the form

$$\left(\frac{q}{q_J}\right)^{\frac{1}{2}} = \frac{K}{(R/D_J)^n} \qquad \ldots\ldots(1)$$

are seen, within limits, to fit the experimental points. In front of the jet, K is about 1 and n increases with α from $n \simeq 1$ at $\alpha = 0^\circ$ to $n \simeq 2.5$ at $\alpha = 50^\circ$. At angles much greater than 50° the entrainment effect of the jet was large enough to prevent any forward spread of the flow from the jet after it has impinged on the ground. Behind the jet, n is about 1 but K increases with inclination of the nozzle from K = 1 at $\alpha = 0^\circ$ to K = 3 at $\alpha = -60^\circ$. The limit of this trend might be seen as K = 6 when $\alpha = -90^\circ$, representing the decay of velocity at the axis of a jet discharging into free air.

Several tests were carried out with an inclined single nozzle to investigate the effect of the height above the ground and results of such tests for two angles are shown in Figures 5 and 6. It had been found in earlier tests[1] that if conditions were related to the pressure of the jet at the point of impingement instead of to the dynamic pressure at nozzle exit then the same equation for the decay would hold provided that the distance R was expressed in terms of the effective diameter of the jet at impingement D_e. Approximately, $D_e = S/6$ (for $S > 6\ D_J$), where S is the slant height of the nozzle exit (Figure 3). Hence Equation (1) becomes:

$$\left(\frac{q}{q_o}\right)^{\frac{1}{2}} = \frac{K}{(R/D_e)^n} \qquad \ldots\ldots(2)$$

Now for a free jet[1]

$$\left(\frac{q_o}{q_J}\right)^{\frac{1}{2}} = \frac{1}{S/6D_J} \text{ for } S > 6\ D_J \qquad \ldots\ldots(3)$$

Equations (2) and (3) give

$$\left(\frac{q}{q_J}\right)^{\frac{1}{2}} = \frac{K}{(R/D_e)^n} \times \frac{1}{S/6D_J} = \frac{K\,(S/6D_J)^{n-1}}{(R/D_J)^n} \qquad \ldots.(4)$$

for $S > 6D_J$.

Equation (4) suggests that when n = 1, as with a vertical jet or in the region behind an inclined jet, test points for different nozzle heights will fall on a common line i.e., there will be no apparent effect of nozzle height. Figure 5 shows such results for a nozzle inclined at 45° and the above tendency is shown, at points distant from jet impingement. There is however an effect of nozzle height ($S > 6D_J$) on the dynamic pressure near the point of jet impingement and it can be seen that q approaches the value of q_o given by Equation (3).

Where n is greater than 1 (in front of the inclined jet) the straight line characteristics are separated but are parallel for any one nozzle angle. The amount of separation depends on the slant height of the nozzle and in the far field $\left(\frac{q}{q_J}\right)^{\frac{1}{2}}$ increases with nozzle height. Figure 6 shows dynamic head readings in front of a jet inclined at 40° to the vertical. For the case where $S/D_J = 24.1$, according to Equation (4) the straight line part of the characteristic will be:

$$\left(\frac{q}{q_J}\right)^{\frac{1}{2}} = \frac{1}{(R/D_J)^{1.73}}\,(24.1/6)^{0.73} = \frac{2.76}{(R/D_J)^{1.73}}$$

This line is drawn on Figure 6 and fits the observations very well at distances of R/D_J greater than 6. Nearer the point of impingement the values of $\left(\frac{q}{q_J}\right)^{\frac{1}{2}}$ tend towards the limits defined by Equation (3).

Similar tests to those on the single nozzle were carried out using the twin nozzle arrangement shown in Figure 1(a). Dynamic head measurements were made near the ground in a plane equidistant from both nozzles. As in the case of the single jet, the dynamic head in front of the jet decreases with nozzle inclination and behind the jet it increases (Figure 7). In front of the jets the maximum dynamic head decays much less rapidly with distance than it does in the case of the single jet, but behind the jets the rate of decay is about the same as that for the single jet. Figure 8 shows the effect of increasing the height of the vertical twin nozzles from 4 D_J to 20 D_J and, rather surprisingly, in the further field, velocities increased with nozzle height. This could possibly be due to the fact that the two jets in the higher position were able to coalesce to form a relatively stronger jet, but from the lower position the jets impinged separately and interfered with each other.

2.2 Decay of maximum temperature after jet impingement

Maximum temperatures in the flow near the ground were measured for single and twin nozzles in both vertical and inclined configurations.

The temperatures at further field points where the velocities and temperatures were low were measured using copper constantan suction thermocouples, using a sensitive galvanometer recorder to measure the e.m.f. Temperatures nearer the point of impingement of the jet were measured using a chromel/alumel non-suction thermocouple, connected to a potentiometer: the nozzle exit total temperature was also monitored.

Plots of θ/θ_J versus R/D_J for the single 2 in. nozzle at various inclinations are shown in Figure 9. The effect of raising the nozzle at a constant inclination is shown in Figures 10, 11 and 12. At far field positions temperatures do not vary much with nozzle height, but near the point of impingement they approach values appropriate to a free jet.

3.0 Taxiing model tests

3.1 Forward extent of jets

A diagrammatic sketch of the rig is shown in Figure 14. The upstream line included a combustion chamber in order that temperature effects could be studied.

The compressed air was led along a pipe, rotating in a horizontal plane near the ground, and was made to impinge on the ground through the nozzle arrangement. By means of a pair of handles the nozzle arm could be rotated manually round a circle of about 11 ft radius. The range of speed at the nozzle was from 5 ft/s to 17 ft/s, and could be held at a steady value over distances of about 30 feet.

Initial tests were carried out with the 1 in. single nozzle mounted vertically at a height of about $4D_J$ above the ground. With the nozzle blowing, the arm was rotated manually and the forward extent of the jet was visualized by the entrainment of a trail of French chalk which had previously been laid in the path of the jet. A cine camera mounted on the arm near the centre of rotation recorded the extent of the dust cloud, which was evaluated from the film by comparison with a grid attached to the nozzle arm, near the nozzle. A typical shot from the cine film is shown in Figure 13 together with a general view of the nozzle arm assembly.

At its outer end, the pipe was supported by a small wheel. A cam on this wheel actuated a microswitch in the circuit of a galvanometer recorder, enabling the forward speed of the nozzle, U, to be measured. The relationship between the observed forward extent of the jet, R_x, and the forward speed is shown in Figure 15(a). The factor U/V_J correlated results for various values of U and V_J when the jet was cold but the results for the hot jet lie off the curve. If the observations are plotted using ratios of dynamic pressures, as in Figure 15(b), a much better correlation results. Hence the parameter defining the extent of the jet is $\left(\frac{q_U}{q_J}\right)^{\frac{1}{2}}$ and not U/V_J. With the nozzle height less than $6D_J$ a series of tests were carried out with the nozzle inclined to the vertical, forwards and backwards, and the forward extent was measured for a range of values of U and V_J.

The double nozzle arrangement was then tested in the same manner as the single nozzle above and all the results are plotted in Figure 17. The

graph shows that the jet(s) extend forward to a point (R_X) at which the maximum dynamic head for the stationary nozzle arrangement would be four times the dynamic head of the still air (q_U) relative to the moving nozzles (see Figure 16). The results, which include hot test runs with the single nozzle vertical, show a pattern consistent with U/V_X having a value of about 0.5.

Four test points have also been added which are derived from full scale tests using a vertically mounted engine in a taxiing aeroplane[3] and are seen to correlate well with the small scale test data.

The rotating nozzle arm was raised to a height of approximately 20 in. and several runs were made with the vertical single and double nozzles. The results have also been plotted in Figure 17, and at low values of U/V_J there is seen to be no effect of height but at larger values the jet is deflected by the motion of the nozzles and consequently lower values of $\sqrt{q_U/q_X}$ are obtained.

3.2 Vertical extent of jets

From the cine film mentioned in Section 3.1 measurements were made of the height of the exhaust cloud above the nozzle. For the single and the double nozzle over the range of inclinations tested the ratio of the upward extent of the exhaust cloud to the forward extent was between $\frac{1}{2}$ and 1. Results of several tests are shown in Figure 18. For the double nozzle the ratio is nearer 1 but for the single it is nearer $\frac{1}{2}$.

4.0 Transient tests

4.1 Growth of jet. Static nozzle arrangement

Earlier work[1] on the vertical 1 in. and 2 in. nozzles included tests in which a hot jet was suddenly turned on and the progress of the hot gas front across the ground was measured by suction couples connected to a galvanometer recorder. The velocity of this front was found to be approximately $\frac{1}{4}$ of the steady state values.

A similar set of tests was made in which the 2 in. nozzle, instead of being turned on suddenly, was swivelled in a vertical plane from a horizontal position to a vertical one, about an axis 6 in. above the nozzle exit. (Axis height $\simeq$ 8 inch.) The velocity u of the hot wave front was measured from tangents to the distance time graphs, two of which are shown in Figure 19. The angular movement of the nozzle was measured on the galvanometer recorder by means of a potentiometer linked to the nozzle. This angular movement is also plotted on Figure 19. It was noticed that if the nozzle was rotated in less than 1 second (model time) the hot gas appeared to start from R = 0 when the angle of the nozzle to the vertical was about 30° (i.e., $\phi = 60^\circ$).

Figure 20 shows several of the tests in which the nozzle was rotated in less than 1 second*. The chosen time scale is $t - t_{30}$ where t_{30} is the time at which the nozzle inclination is 30° to the vertical. The

* $$\text{Full-scale time} = \text{model time} \times \left(\frac{D_J}{\sqrt{q_J}}\right)_{F.S.} \times \left(\frac{\sqrt{q_J}}{D_J}\right)_{model}$$

results agree well with the curve calculated using the $\frac{1}{4}$ steady state velocity rule (see Appendix II), and so the effect is seen to be the same as if the jet had been fixed in a vertical position and suddenly turned on at time t_{30}.

Test points for a case where the nozzle was rotated slowly are shown in Figure 21. In this case the jet appears to start at R = 0 when $\phi = 40$ ($\alpha = 50$). An attempt was made to synthesize such a transient using steady state readings for different nozzle inclinations and the 4/1 relationship between steady state and transient velocities or, strictly speaking, the 16/1 relationship between steady state and transient dynamic heads (see Appendix II). Figure 21 shows that the "built up" transient fits the experimental points fairly closely.

Several tests were made in which the 2 in. nozzle was initially horizontal and was swivelled quickly (in $\frac{1}{2}$ a second or less) to 20° to the vertical; one test was made in which the final angle α was 40°. The rate of progress of the hot wave of gas across the floor was measured and the velocities determined from tangents to the distance time graphs. The results are shown in Figure 22 in the usual way $\left(\left(\frac{q_u}{q_J}\right)^{\frac{1}{2}} \text{ versus } R/D_J\right)$ and are compared with the $\frac{1}{4}$ x steady state values.

4.2 Growth of jet. Taxiing nozzle arrangement

The test rig described in Section 3.1 also had the facility to turn the twin nozzles from the horizontal to the vertical direction as the nozzle arm was traversed across the ground. This was done by means of an hydraulic system operated by a large cam attached to the vertical duct at the centre of rotation of the nozzle arm. By using the French chalk technique described in Section 3.1 the growth of the jet was recorded on the cine film. The rotation of the nozzles was measured by a pointer attached to the nozzles, and a fixed angular scale both of which appeared on the cine film. In several tests one of the nozzles was blanked, so that results were obtained for both single and double nozzle arrangements.

Results of two such tests are shown in Figure 23. The calculated progress of the jet along the ground using $\frac{1}{4}$ x steady state values (Appendix III) is also shown. It can be seen that, as with the stationary nozzle, the exhaust gases appear to start at R = 0 when $\phi = 60°$, that is when the nozzles are at about 30° to the vertical.

5.0 Conclusions

(1) The maximum steady state velocities in the flow near the ground from single and double jets impinging vertically and at an angle to the ground have been measured. It was found that the parameters which best correlated measurements for a wide range of jet velocity and temperature were $\left(\frac{q}{q_J}\right)^{\frac{1}{2}}$ and $\frac{R}{\sqrt{C_D}\, D_J}$; however, in the case of the convergent nozzles used $\sqrt{C_d} \simeq 1$, and $\frac{R}{D_J}$ can be used as the correlating parameter without much error.

(2) The maximum steady state temperatures in the flow near the ground from single and double jets impinging vertically and at an angle to the ground have been measured and the parameters used to correlate measurements for a wide range of jet velocity and temperature were θ/θ_J and R/D_J.

(3) When the nozzles, discharging downwards, were moved parallel to the ground at constant velocity U, the forward extent of the jet flow was to a point where $\left(\frac{q_U}{q_x}\right)^{\frac{1}{2}} \approx 0.5$ (see Figure 17). This was shown to be the case for single and twin nozzles over a wide range of relative speed $\frac{U}{V_J}$, with the nozzles at various inclinations and with heated as well as cold jets. This finding is expressed by the approximate rule, that the flow from a moving jet penetrates upwind to a point where, in a test under stationary conditions, the maximum velocity of the jet would be twice the speed of the relative wind in the moving case.

The height of the exhaust cloud was found to be between $\frac{1}{2}$ and 1 times the upwind extent.

(4) A 4/1 correspondence was found to exist between steady state readings and the transient velocities set up when jets were suddenly swivelled from horizontal to vertical, and from horizontal to an angle α^o to the vertical.

This value confirms that found in Reference 1 where the transient conditions were set up by the sudden turning on of a vertical jet.

It was found that the growth of the jet on swivelling, in the stationary and the moving case, could be predicted with reasonable accuracy using steady state readings and the 4/1 correspondence of steady state to transient measurements.

REFERENCES

No.	Author(s)	Title, etc.
1	M. Cox	Studies of the flow fields created by single vertical jets directed downwards upon a horizontal surface. A.R.C. C.P. 912
2	S. L. Bragg	Effect of compressibility on the discharge coefficients of orifices and convergent nozzles. Journal of Mechanical Engineering Science, March, 1960.
3	-	Unpublished work at Messrs. Rolls-Royce Ltd.

APPENDIX I

Nomenclature

C_D	discharge coefficient of nozzle = $\frac{\text{mass flow at nozzle exit}}{\text{maximum velocity} \times \text{density} \times \text{area}}$
D_c	effective diameter of nozzle exit ($\sqrt{C_D} \times D_J$)
D_J	geometric diameter of nozzle
D_e	effective diameter of jet at impingement
H	vertical height of nozzle exit
h	height of exhaust cloud above nozzle
S	slant height of nozzle exit (H/cos α)
R	distance from point of jet impingement
R_x	forward extent of jet from point of jet impingement
T	total temperature (local)
T_a	ambient temperature
T_J	nozzle exit total temperature
θ	$T - T_a$
θ_J	$T_J - T_a$
ρ_a	air density (ambient)
U	velocity of nozzle(s) along ground
q	local dynamic head (total pressure - static pressure)
q_J	dynamic head of jet at nozzle exit
q_o	pressure head in stagnation region at point of jet impingement
q_U	dynamic head of still air relative to moving nozzle ($\frac{1}{2}\rho_a U^2$)
q_x	dynamic head of jet from static nozzle at distance R_x
q_u	dynamic head of transient hot wave front ($\frac{1}{2}\rho_a u^2$)
V_J	velocity of jet at nozzle exit
u	transient velocity of hot wave front
α	inclination of nozzle to vertical (positive if nozzle points backwards relative to aircraft motion)

ϕ inclination of nozzle to horizontal (90 - α)

t time, (second)

t_o time of swivel of nozzle from horizontal to vertical direction

t_{30} time of swivel of nozzle from horizontal to angle of 30^o to vertical

APPENDIX II

To obtain transient growth of jet from steady state readings. Static single nozzle rotated from horizontal

For an inclined nozzle the steady state dynamic head readings (in front of the jet) are related to radial distance by:-

$$\left(\frac{q}{q_J}\right)^{\frac{1}{2}} \doteq \frac{1}{(R/D_J)^n} \quad \text{where n varies with } \alpha \text{ (Section 2.1)}$$

Using a 4/1 correspondence between steady state and transient conditions:-

$$\left(\frac{q_u}{q_J}\right)^{\frac{1}{2}} = \frac{1}{4}\frac{1}{(R/D_J)^n} \qquad \ldots.(1)$$

$$\therefore \quad u = \frac{(q_J)^{\frac{1}{2}}}{4\sqrt{\frac{1}{2}\rho}} \frac{1}{(R/D_J)^n} = \frac{dR}{dt}$$

$$\therefore \quad \frac{R^n dR}{dt} = \frac{D_J{}^n \, q_J{}^{\frac{1}{2}}}{4\sqrt{\rho/2}}$$

integrating we get

$$\therefore \quad R^{n+1} = \frac{(n+1)\, D_J{}^n \, (q_J)^{\frac{1}{2}}}{4\sqrt{\rho/2}} (t - t_{3o}) \qquad \ldots.(2)$$

Equation (1) for $\alpha = 20^o$ and $\alpha = 40^o$ is plotted in Figure 22.
Equation (2) is plotted in Figure 20, and compared with results from tests in which the nozzle was rotated from horizontal to vertical in less than a second.

For the cases where the nozzle was rotated slowly (e.g., Figure 21) the transients were synthesized using $\frac{1}{4}$ × steady state values, as follows.

In Figure 24 the curve PQ shows the angular movement of the nozzle. At the point A, when $\alpha = 55^o$ the jet impinges at a point R55 away from the point of final jet impingement (when the nozzle is vertical). At B the jet is at 50^o to the vertical and so the curve A B C D represents the movement of the point of jet impingement towards the final position where $\alpha = 0$.

The curve AE is drawn using Equation (2)

$$\text{i.e.,} \qquad (R - R_{55})^{n+1} = \frac{(n + 1)\, D_J^{\,n}\, (q_J)^{\frac{1}{2}}\, (t - t_{55})}{4\, (\rho/2)^{\frac{1}{2}}}$$

using the appropriate value of n for $\alpha = 55^{\circ}$.

At the next interval (i.e., at $\alpha = 50^{\circ}$) the curve B X H is drawn whose equation is

$$(R - R_{50})^{n+1} = \frac{N \times (n + 1)\, D_J^{\,n}\, (q)^{\frac{1}{2}}\, (t - t_{50})}{4\, (\rho/2)^{\frac{1}{2}}}$$

where N is an arbitrary constant having a value between 1 (transient) and 4 (steady state). Where this curve crosses AE at X, the transient or $\frac{1}{4}$ x steady state equation is used to continue the curve but with an origin displaced distance wise from B to U to allow for the distance already covered up to the point X. This curve is U X F.

The above is now repeated for $\alpha = 45^{\circ}$ using $\frac{N}{4}$ x steady state values up to Y and then $\frac{1}{4}$ x steady state values along S Y G and so on until $\alpha = 0$ is reached. The growth of the jet is taken as the envelope of these curves. Values of N of 1 2 3 and 4 were tried for a number of cases and it was found that N = 2 gave the most consistent agreement between observed and estimated curves. One example is shown in Figure 21.

APPENDIX III

To obtain transient growth of jet from steady state readings. Taxiing single and twin nozzle arrangements, rotated from horizontal to vertical suddenly

In the steady state it was found (Section 3.0) that at the jet reversal point the relative cross wind velocity had about twice the effect of the local jet velocity with no cross wind i.e.,

$$\left(\frac{q_U}{q_X}\right)^{\frac{1}{2}} \simeq 0.5 \text{ at } R_X$$

Therefore, when deciding a notional effective velocity in the jet, relative to the point of impingement, we reduce the local jet velocity by twice the relative wind speed, so that effectively

$$\left(\frac{q}{q_J}\right)^{\frac{1}{2}} = \frac{K}{(R/D_J)^n} - 2\left(\frac{q_U}{q_J}\right)^{\frac{1}{2}}$$

and the transient wave front speed using $\frac{1}{4}$ of the above value is

$$\left(\frac{q_u}{q_J}\right)^{\frac{1}{2}} = \frac{1}{4}\left(\frac{K}{(R/D)^n} - 2\left(\frac{q_U}{q_J}\right)^{\frac{1}{2}}\right)$$

$$\therefore \qquad u = \frac{\frac{1}{4}\, q_J K}{(\rho/2)^{\frac{1}{2}}\ (R/D_J)^n} - \frac{U}{2} = \frac{dR}{dt}$$

This expression is not easily integrated analytically and graphical methods were used. A plot of $\frac{1}{u}$ versus R, integrated up to R_2 say, gives the time taken by the jet boundary to reach R_2.

Values obtained by the above method are plotted in Figure 23.

FIG 1.

(b) 2" & 1" DIAMETER CONICAL NOZZLES

a) TWIN CONVERGING NOZZLES (1" DIAMETER)

SCALE : $\frac{1}{2}$ x F.S

NOZZLES TESTED

FIG 2.

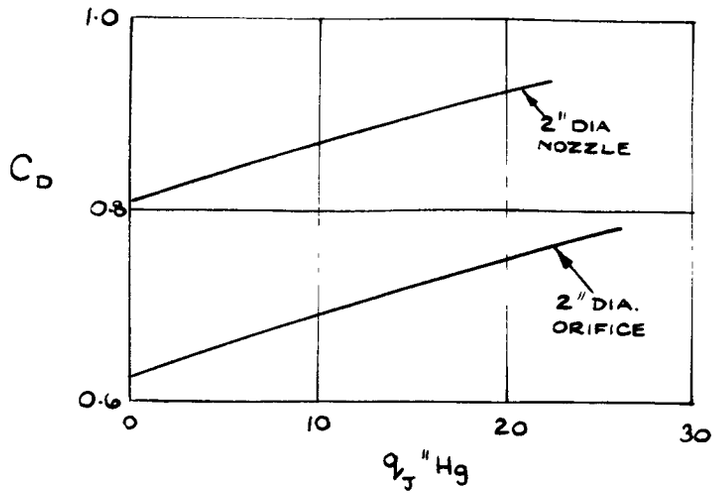

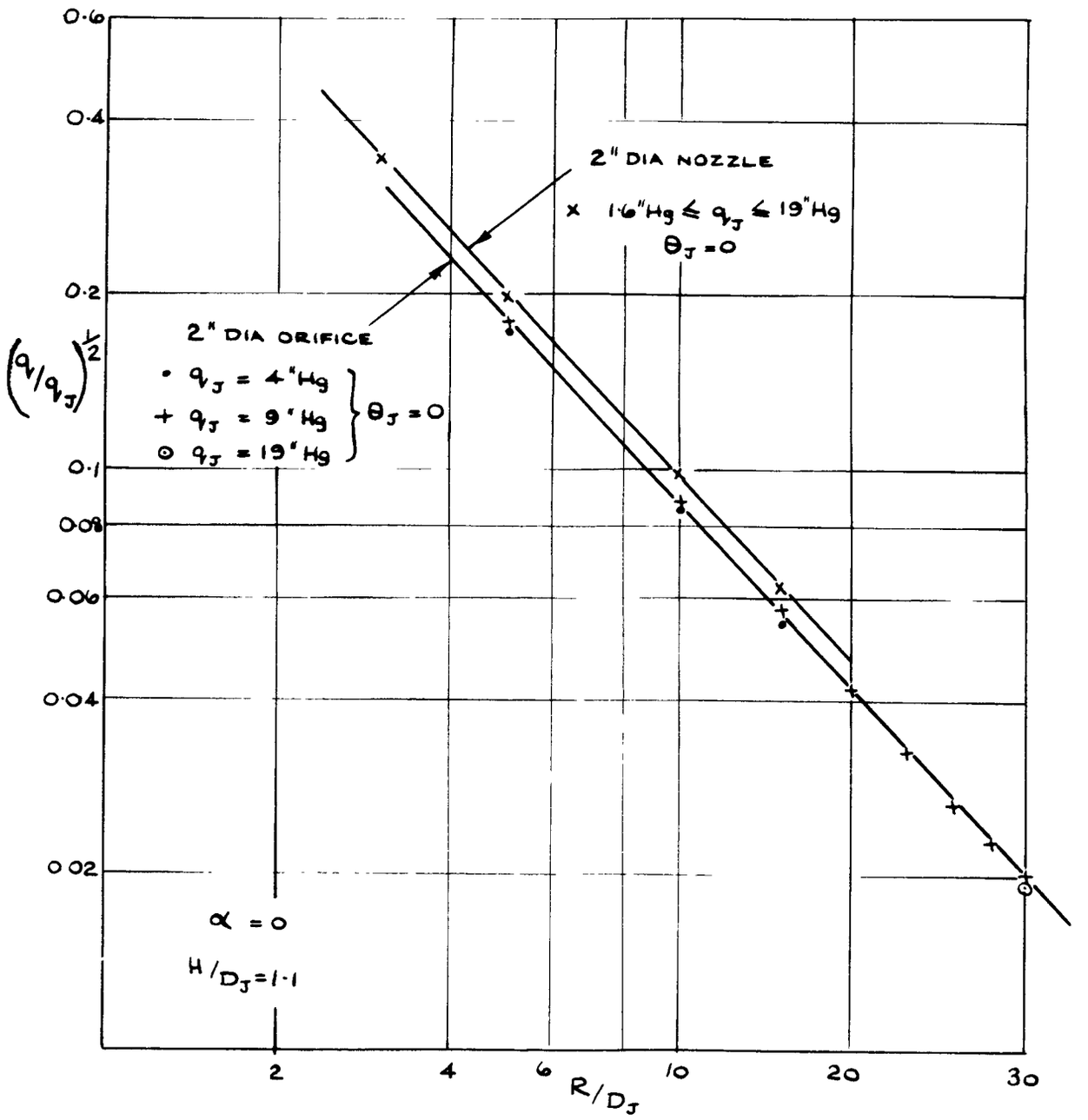

EFFECT OF DISCHARGE COEFFICIENT OF NOZZLE ON DECAY OF MAXIMUM DYNAMIC HEAD

FIG. 3.

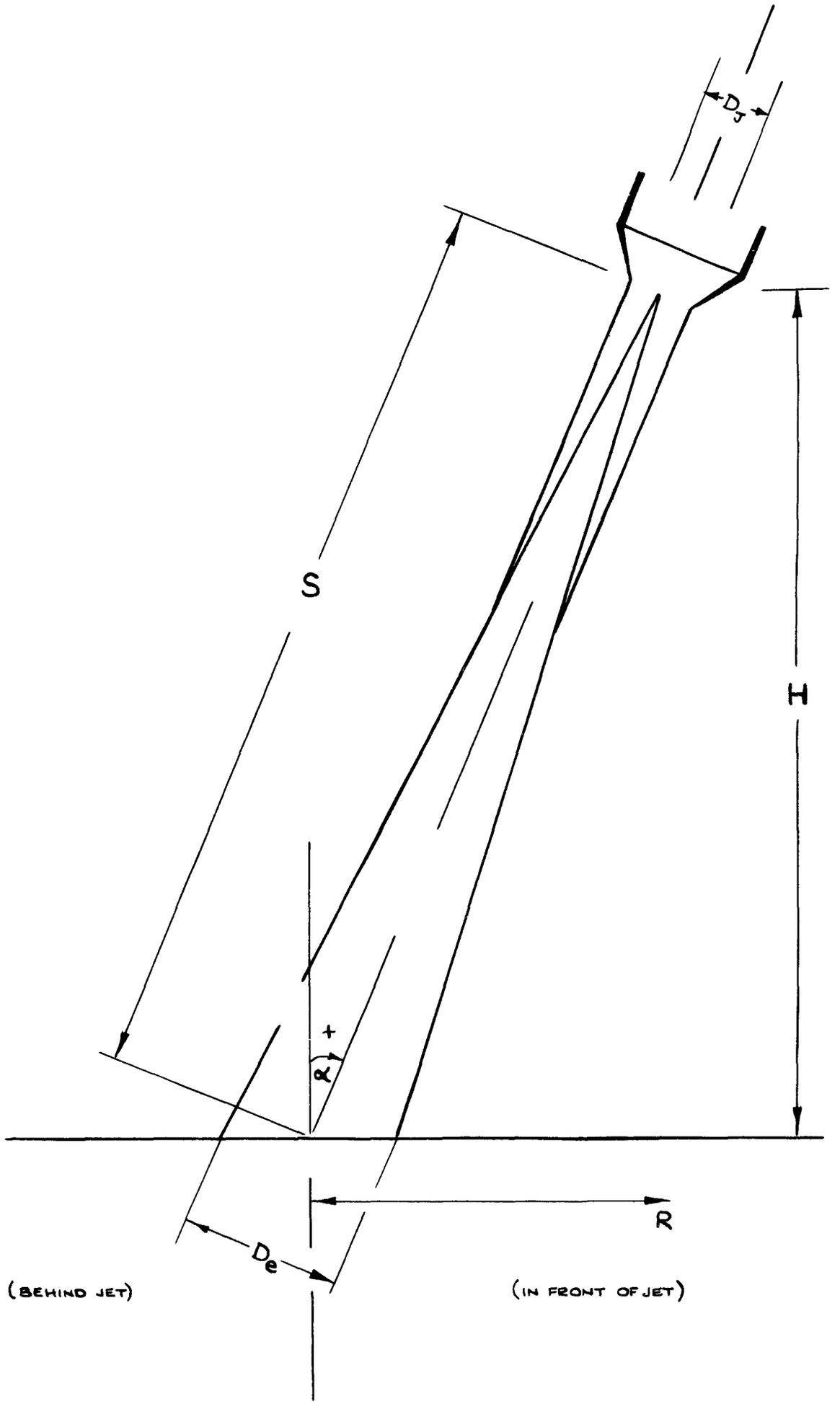

JET GEOMETRY

FIG. 4.

	①	②	③	④	⑤	⑥	⑦	⑧	⑨	⑩
$\alpha°$	0	10	20	33	40	41	50	-20	-45	-60
H/D_J	1·1	1·1	1·3	1·6	1·8	1·8	2·2	1·3	2·0	2·6

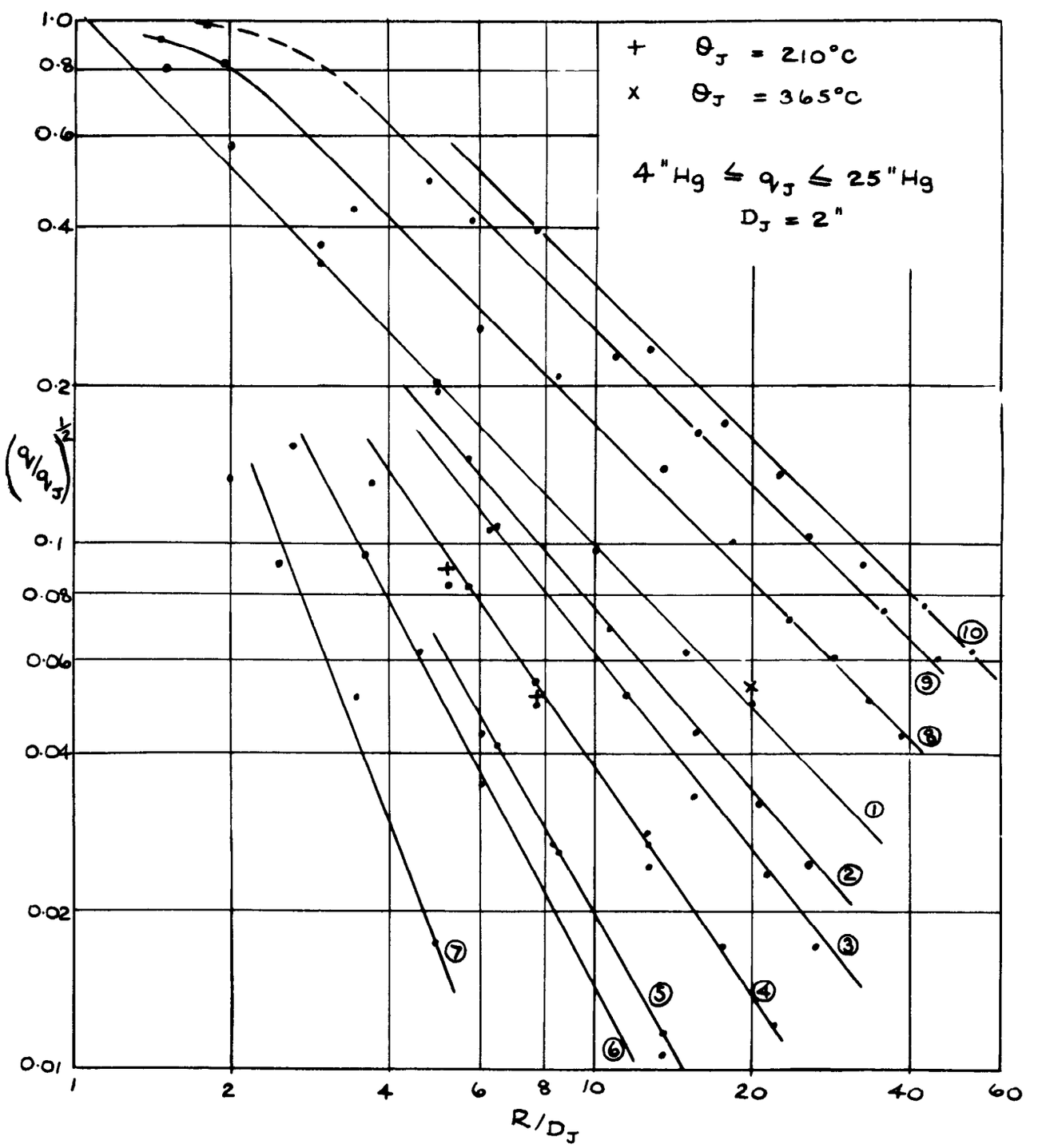

DECAY OF MAXIMUM DYNAMIC HEAD. EFFECT OF NOZZLE INCLINATION. SINGLE NOZZLE $S/D_J < 6$

FIG. 5.

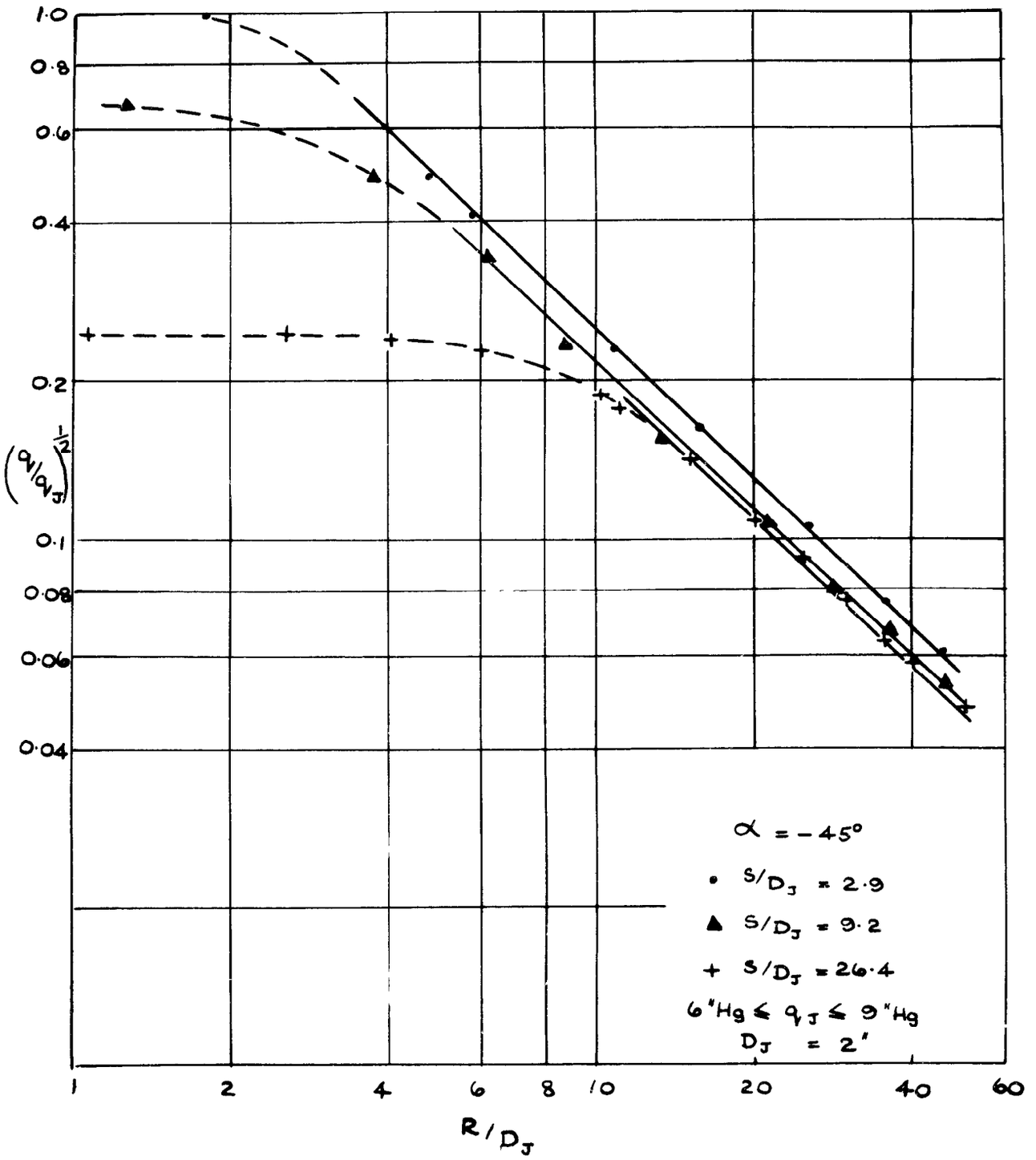

DECAY OF MAXIMUM DYNAMIC HEAD
EFFECT OF NOZZLE HEIGHT
INCLINED SINGLE NOZZLE

FIG.6.

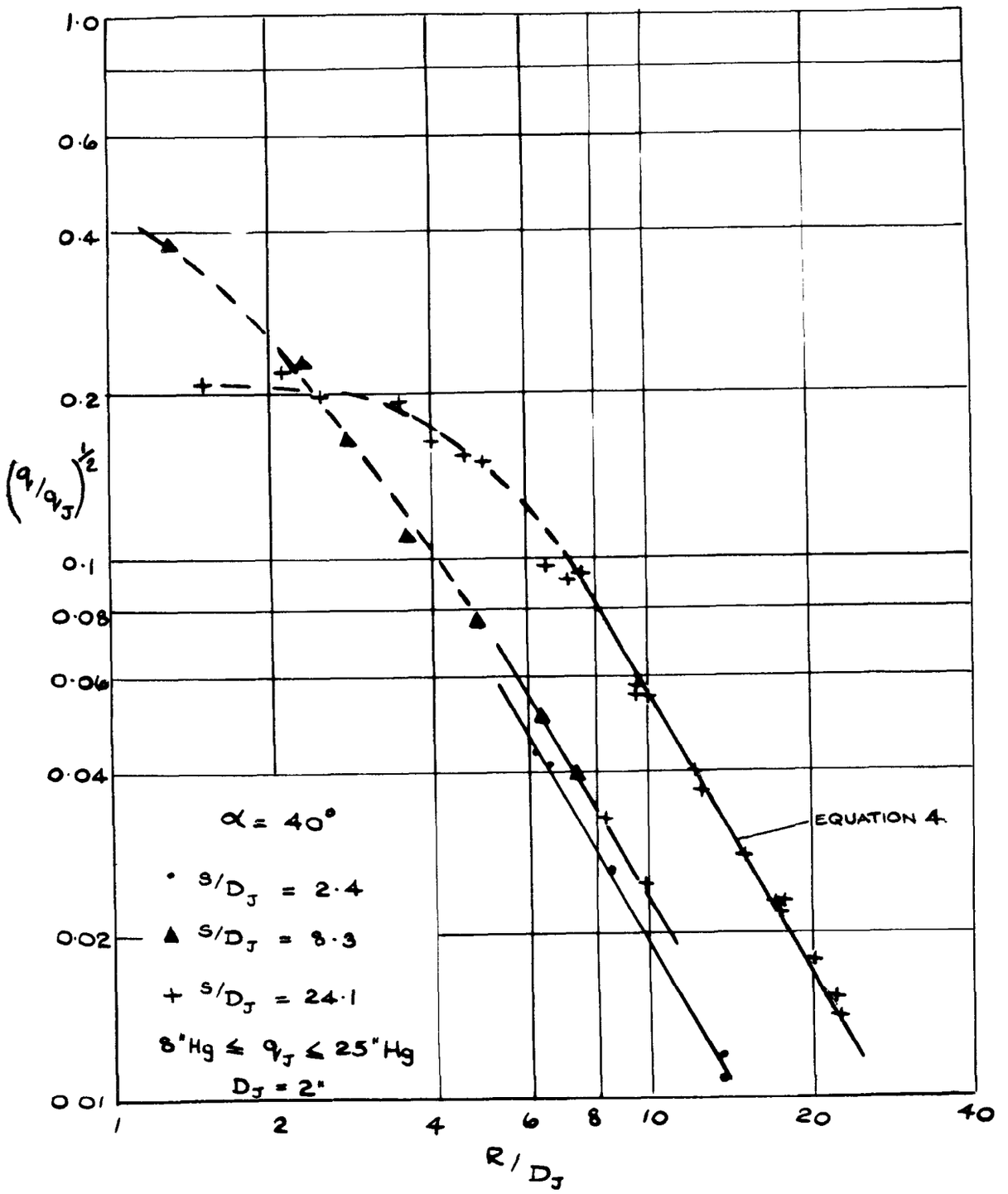

DECAY OF MAXIMUM DYNAMIC HEAD
EFFECT OF NOZZLE HEIGHT
INCLINED SINGLE NOZZLE

FIG. 7.

	①	②	③	④
α	0	10	20	-20
H/D_J	4·2	6·3	4·2	4·2

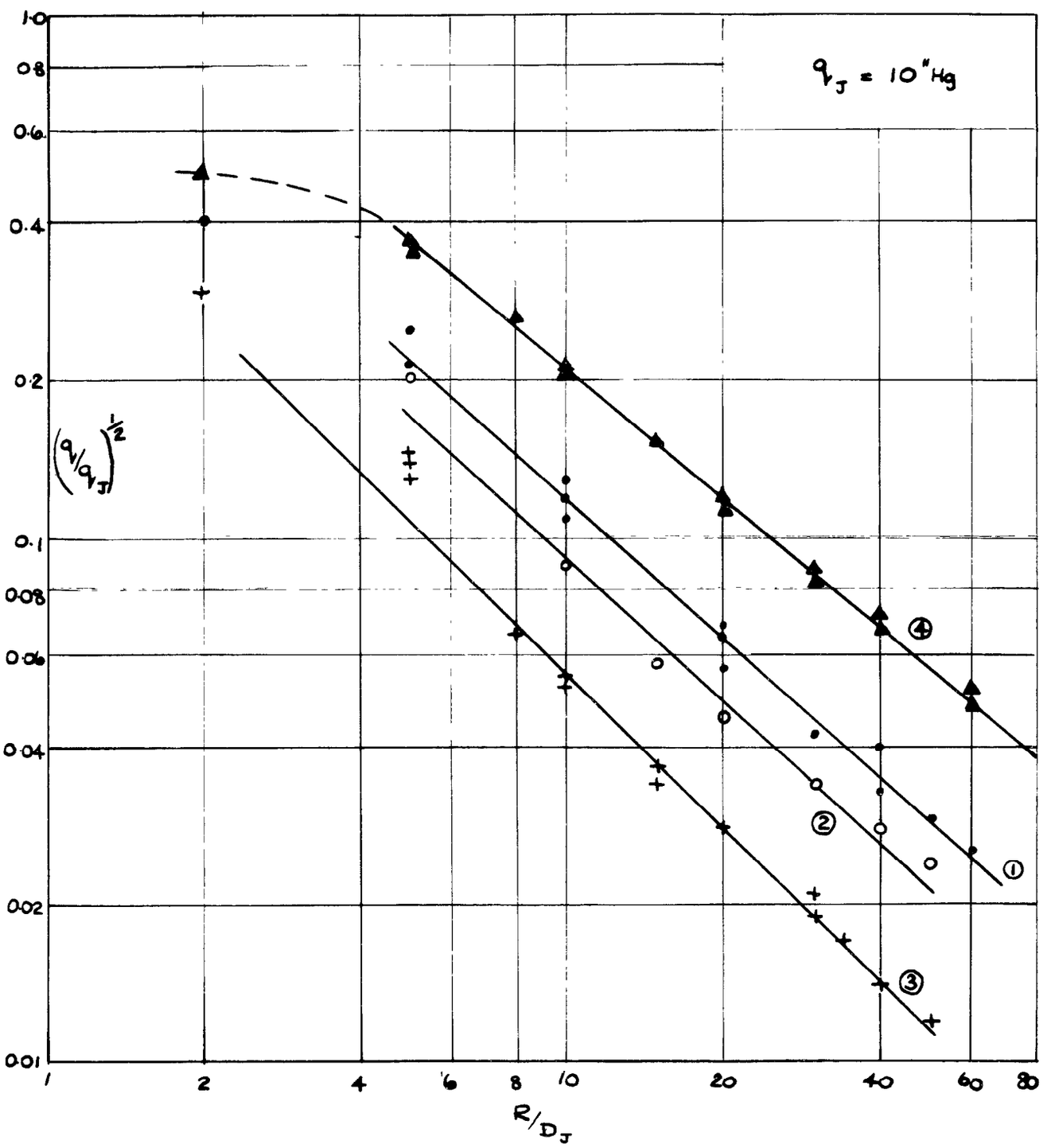

DECAY OF MAXIMUM DYNAMIC HEAD
EFFECT OF NOZZLE INCLINATION
DOUBLE NOZZLE $S/D_J < 7$

FIG.8.

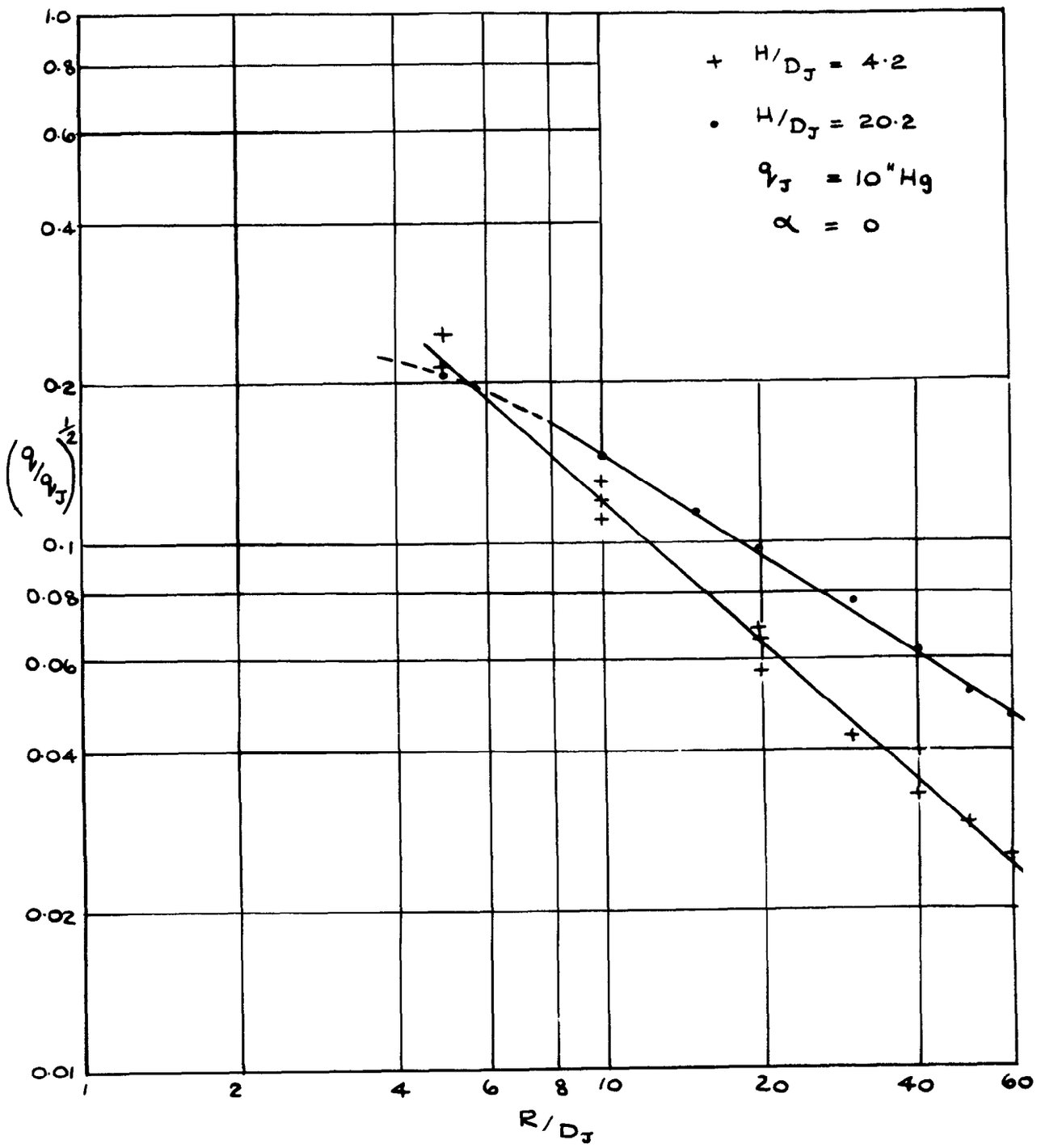

DECAY OF MAXIMUM DYNAMIC HEAD
EFFECT OF NOZZLE HEIGHT
DOUBLE NOZZLE VERTICAL

FIG.9.

	①	②	③	④	⑤	⑥
α	0	20	40	-25	-45	-60
H/D_J	1·1	1·3	1·8	1·4	2·0	2·6

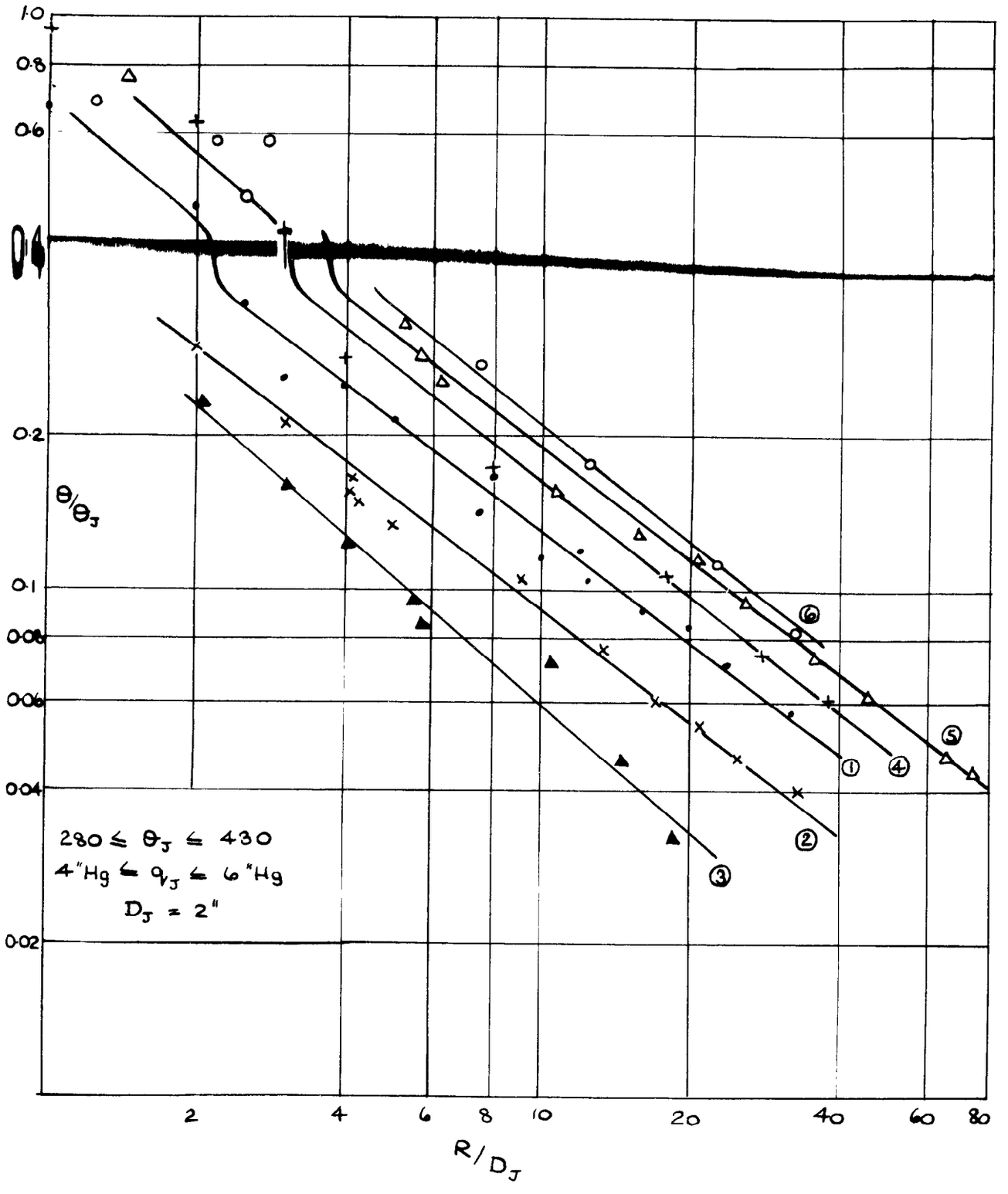

DECAY OF MAXIMUM TEMPERATURE
EFFECT OF NOZZLE INCLINATION
SINGLE NOZZLE $S/D_J < 6$

FIG.12.

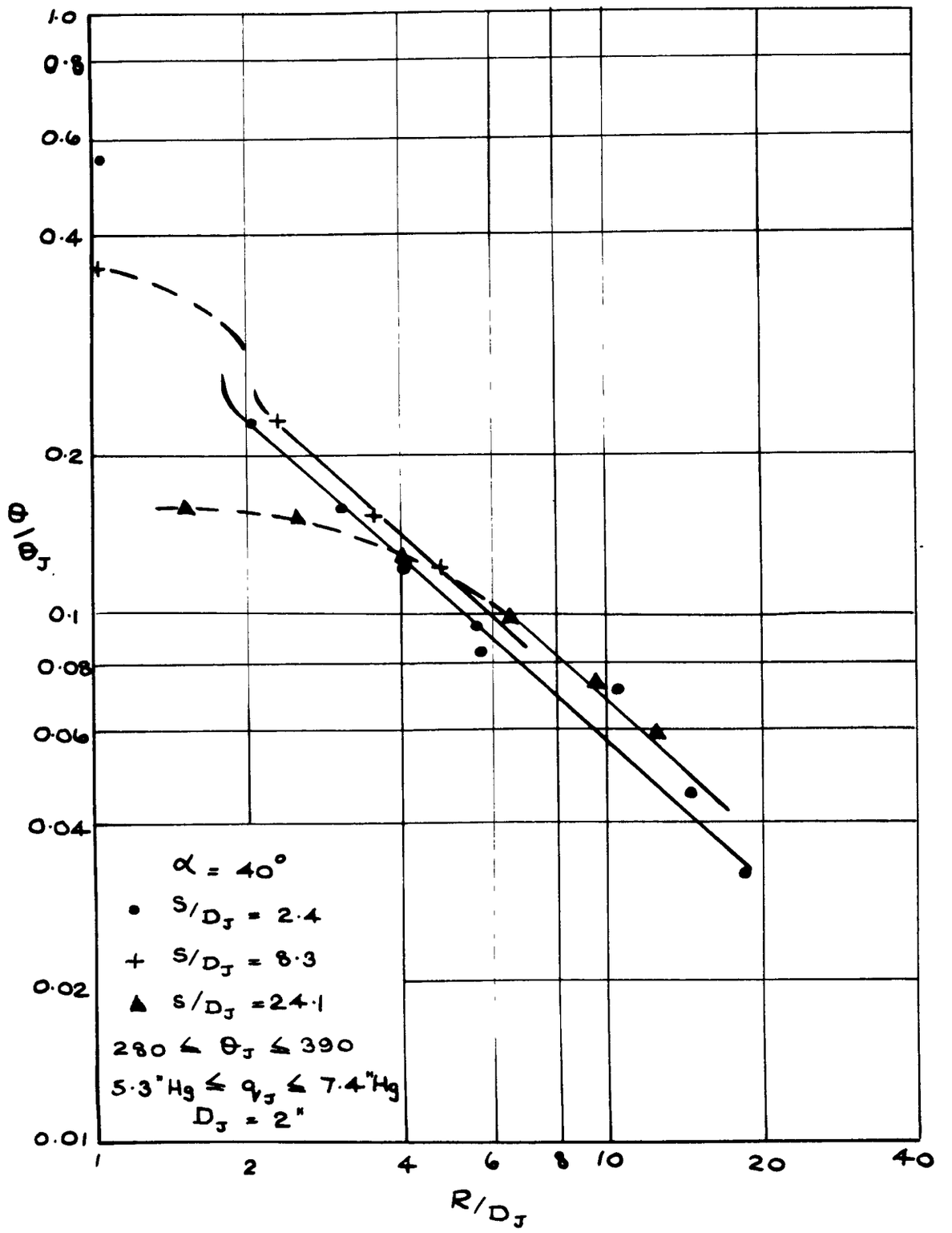

DECAY OF MAXIMUM TEMPERATURE
EFFECT OF NOZZLE HEIGHT
SINGLE NOZZLE INCLINED

FIG.9.

	①	②	③	④	⑤	⑥
α	0	20	40	-25	-45	-60
H/D_J	1·1	1·3	1·8	1·4	2·0	2·6

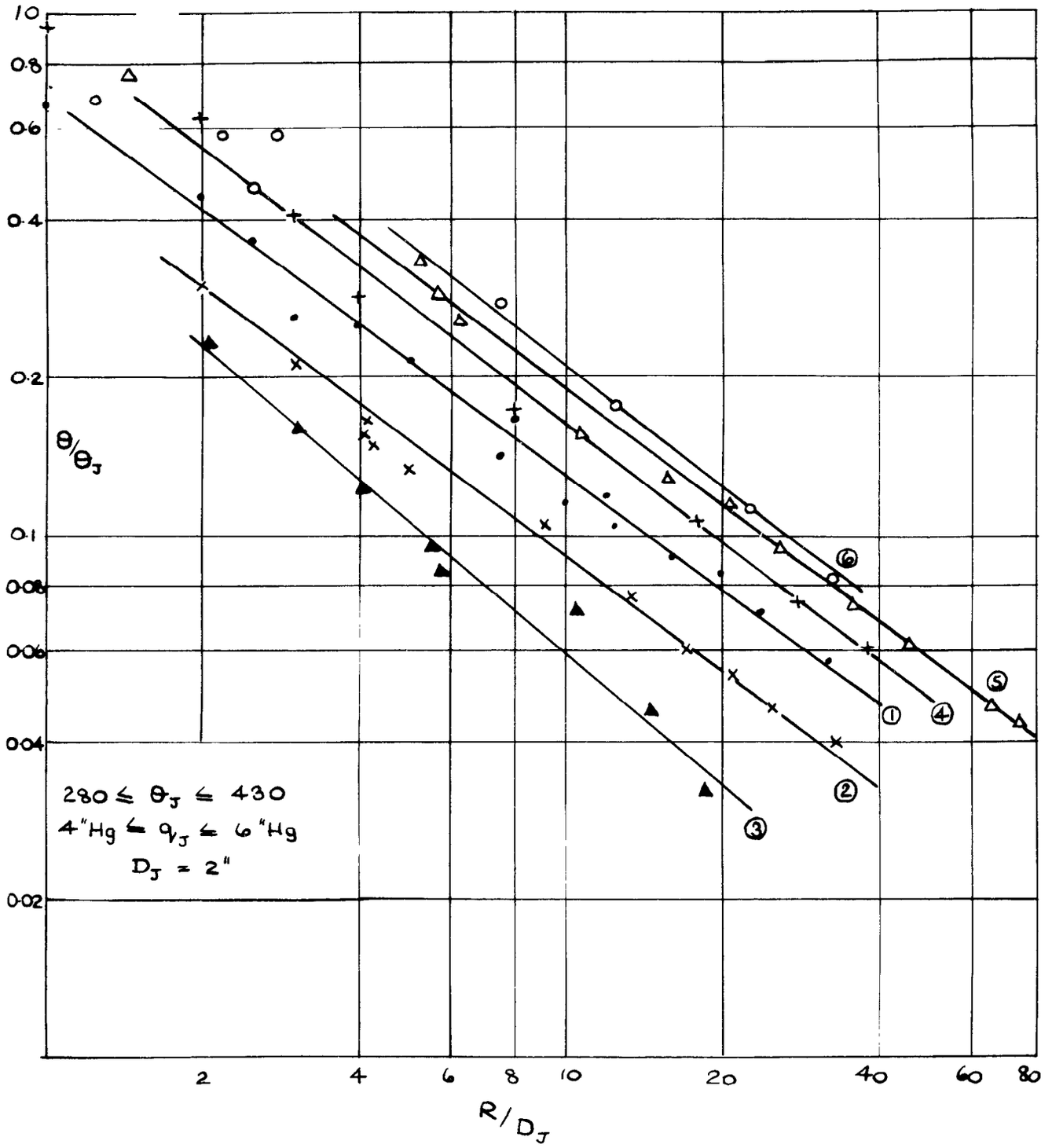

DECAY OF MAXIMUM TEMPERATURE
EFFECT OF NOZZLE INCLINATION
SINGLE NOZZLE $S/D_J < 6$

FIG.10.

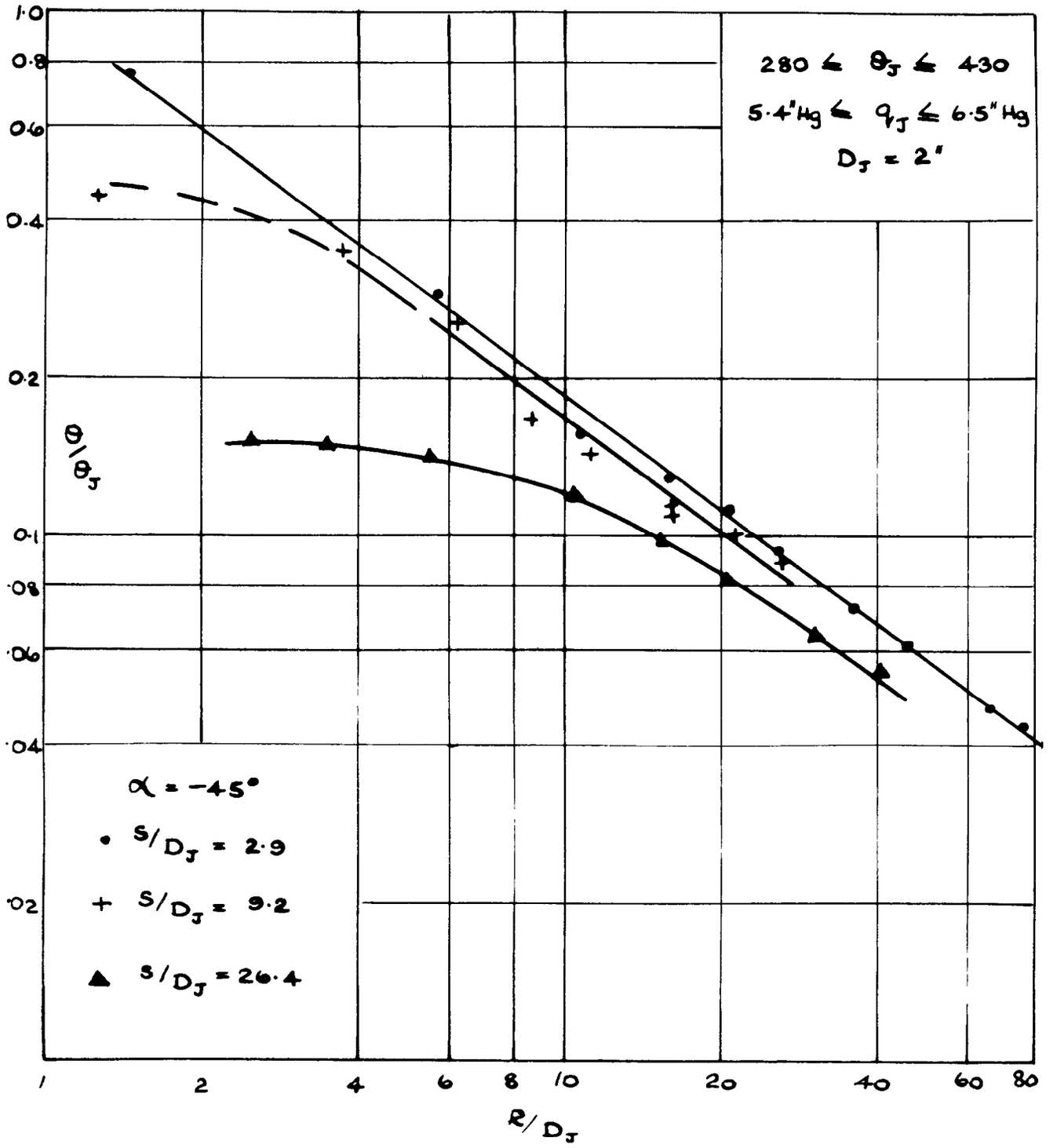

DECAY OF MAXIMUM TEMPERATURE
EFFECT OF NOZZLE HEIGHT
SINGLE NOZZLE INCLINED

FIG.11.

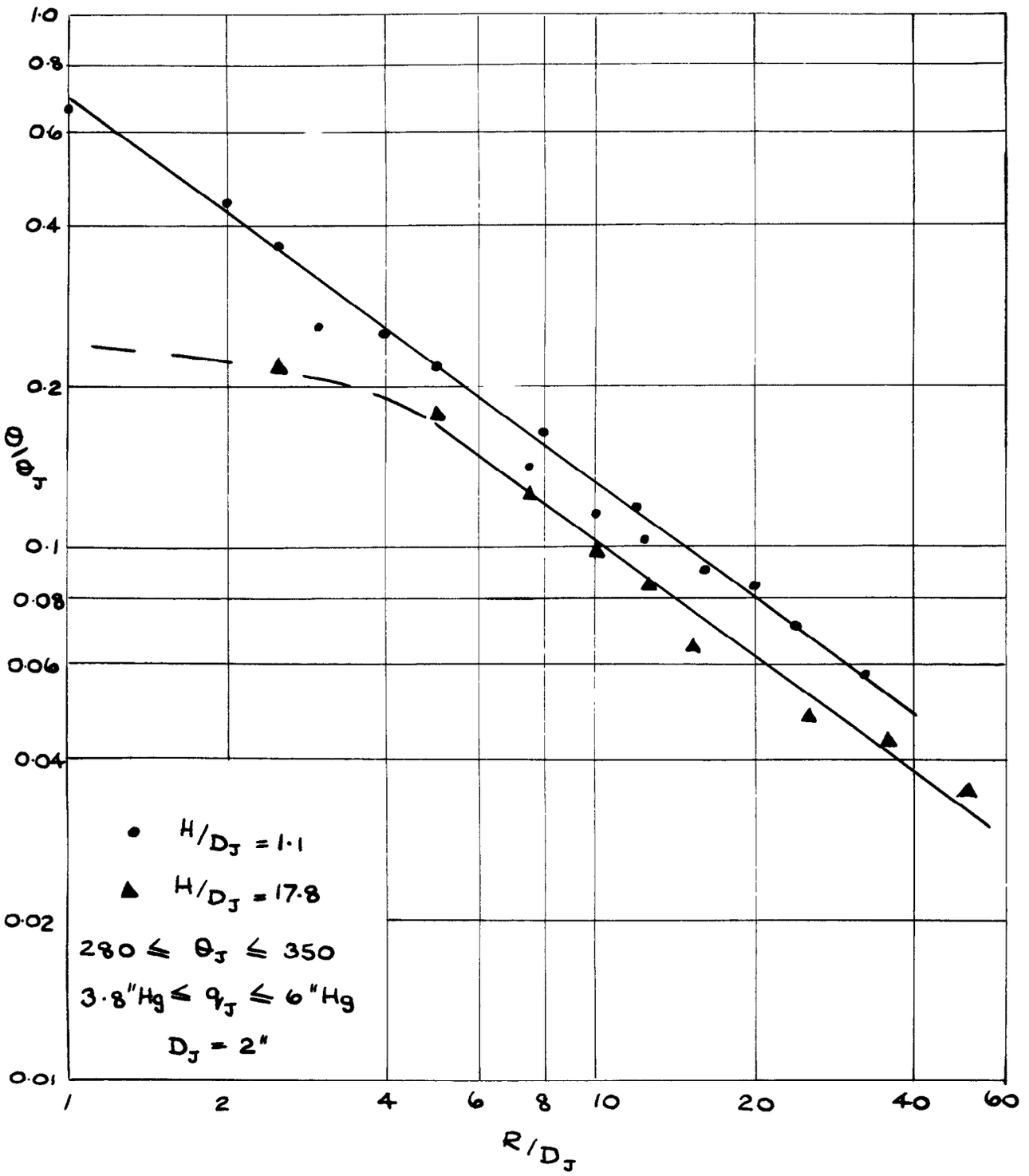

DECAY OF MAXIMUM TEMPERATURE
EFFECT OF NOZZLE HEIGHT
SINGLE NOZZLE VERTICAL

FIG.12.

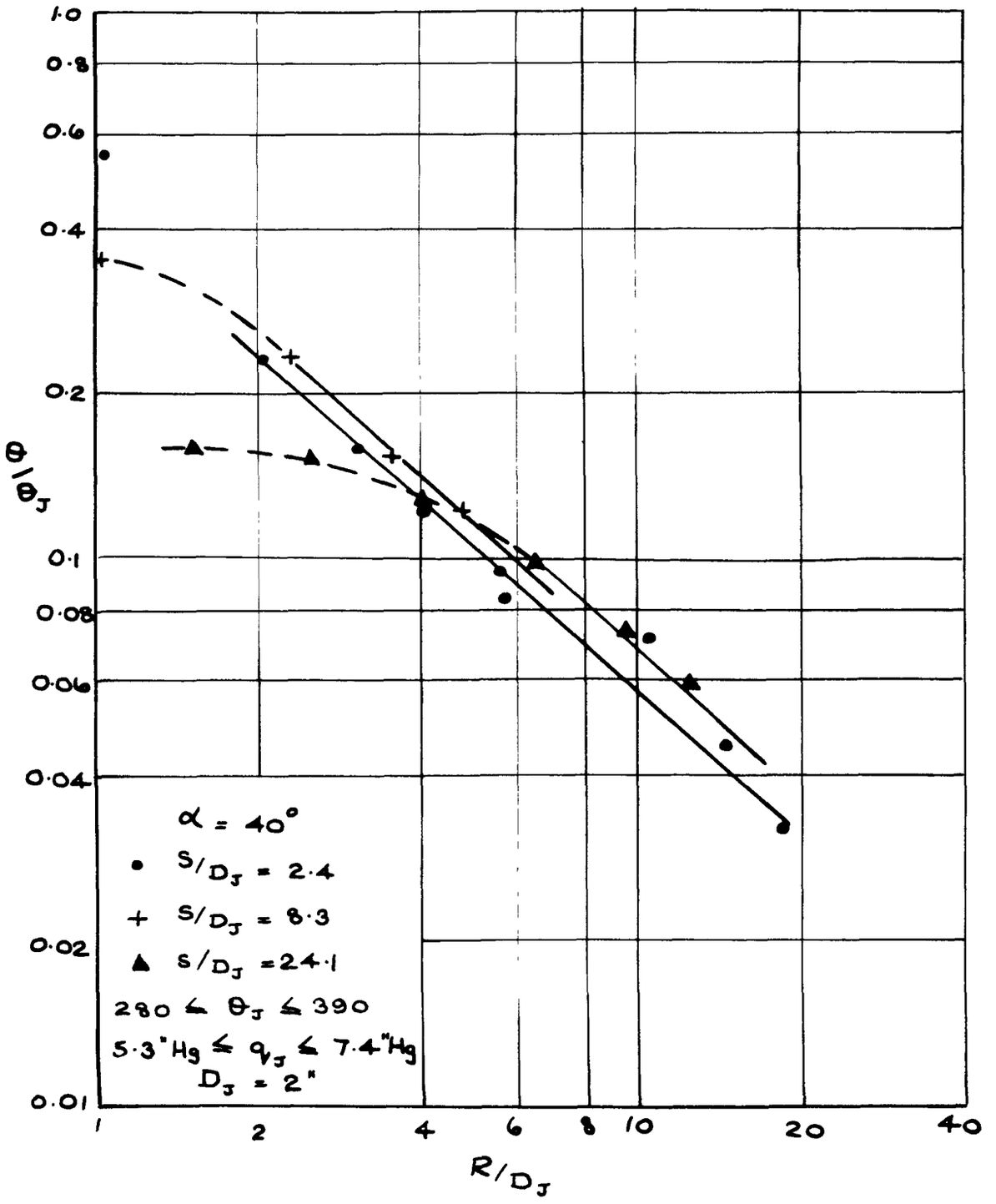

DECAY OF MAXIMUM TEMPERATURE
EFFECT OF NOZZLE HEIGHT
SINGLE NOZZLE INCLINED

FIG. 13.

REP. 14-64

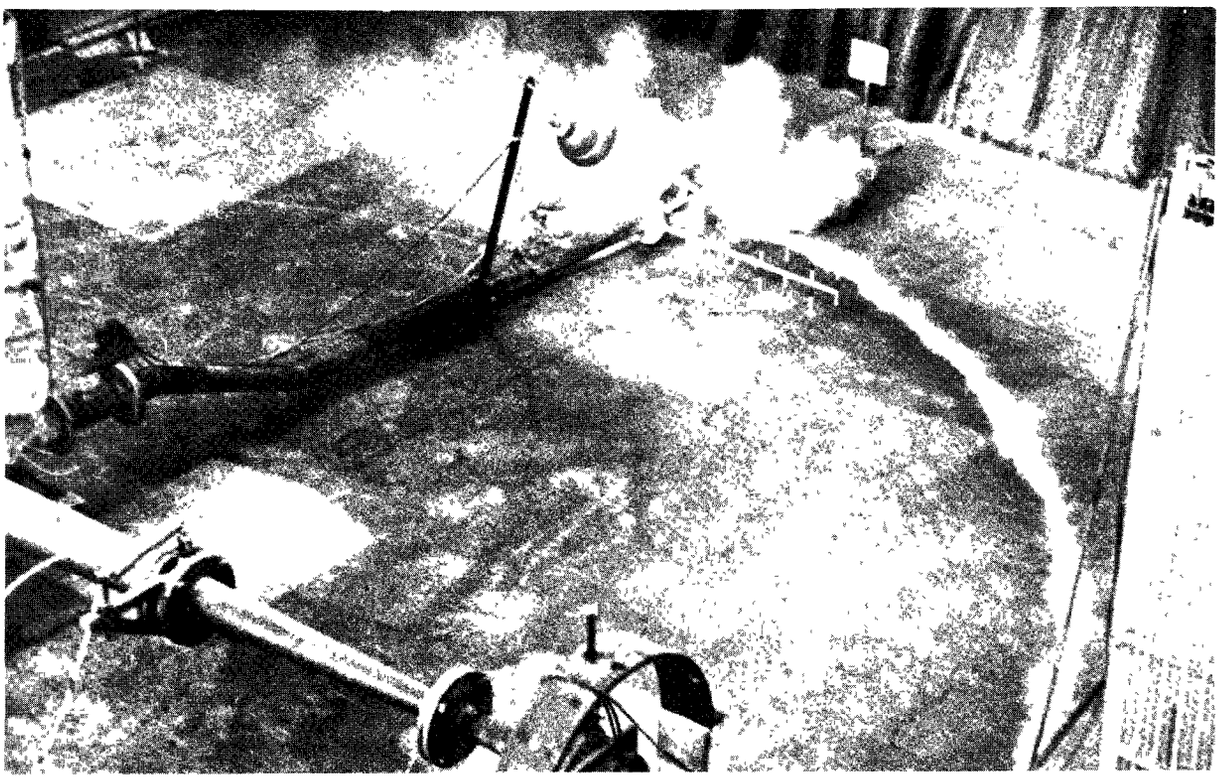

ROTATING NOZZLE ARM

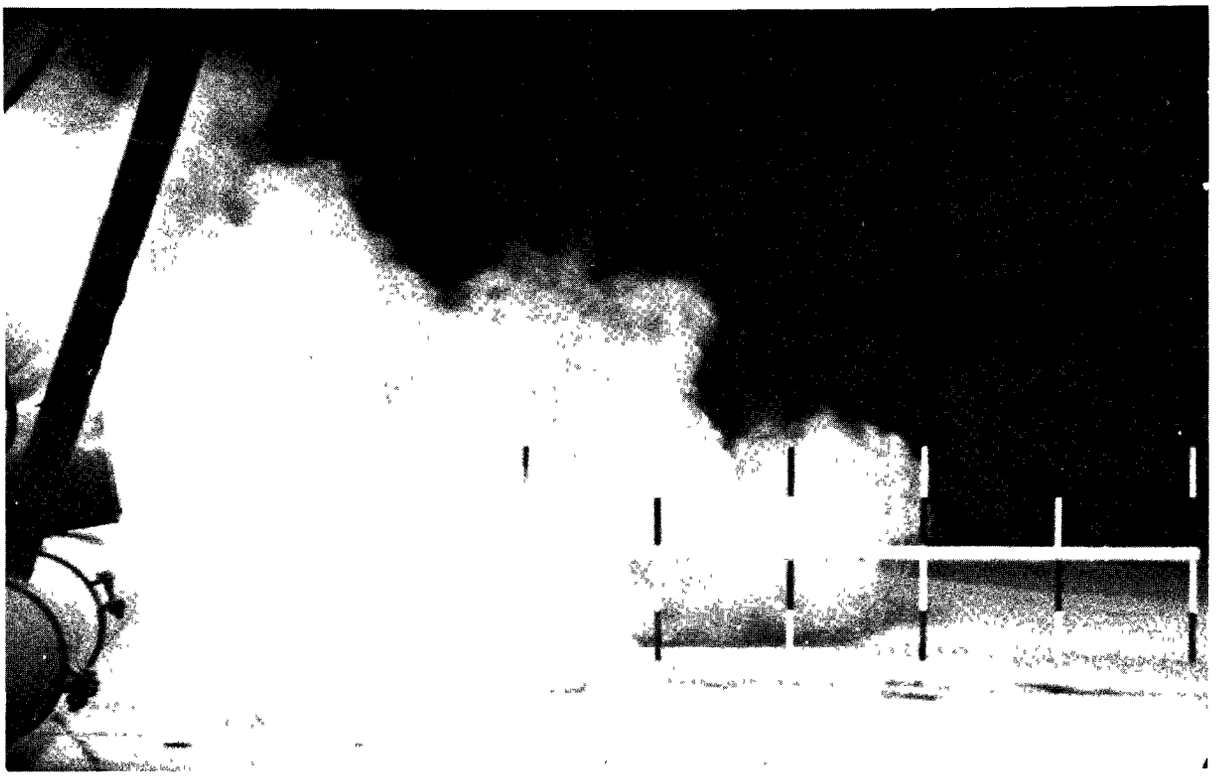

MEASUREMENT OF EXTENT OF MOVING JET

FIG.14.

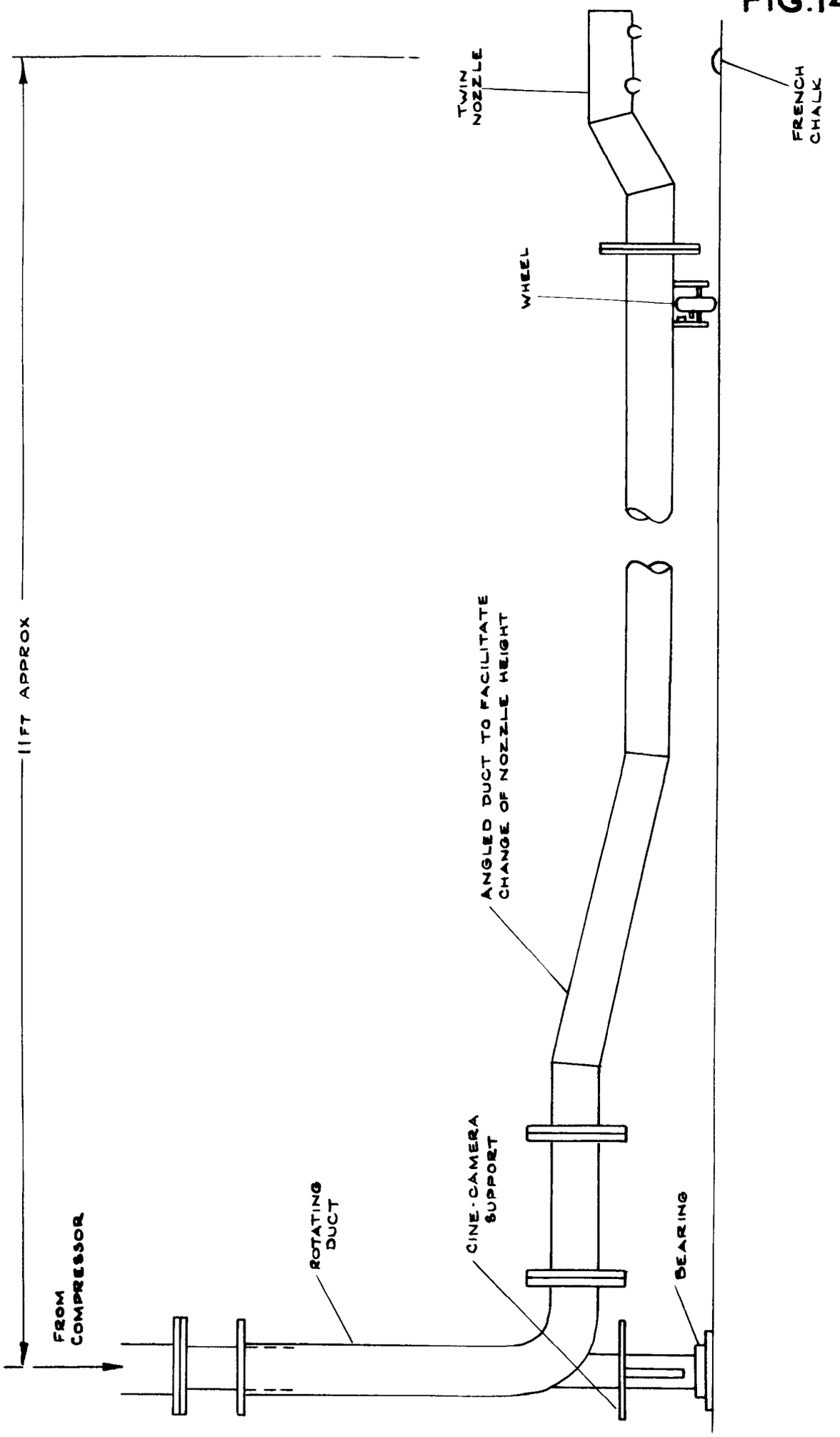

TEST RIG FOR TAXIING MODEL NOZZLES

FIG. 15.

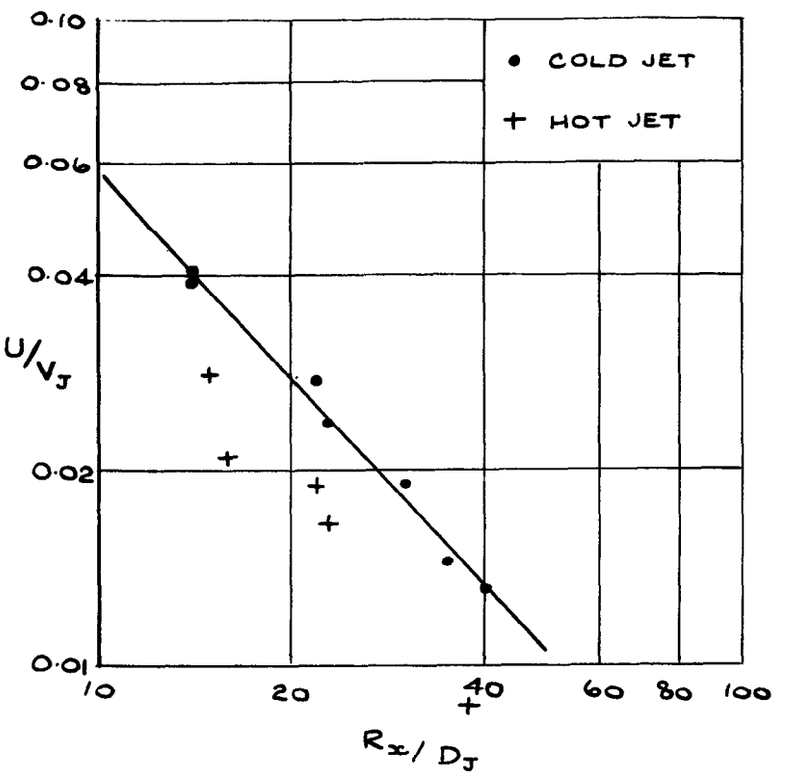

15a

$D_J = 1'$ 4 FT/SEC $\leq U \leq$ 17 FT/SEC.

$6"H_2O \leq q_J \leq 6"Hg$ $160°C \leq \theta_J \leq 320°C$

$H/D = 4$

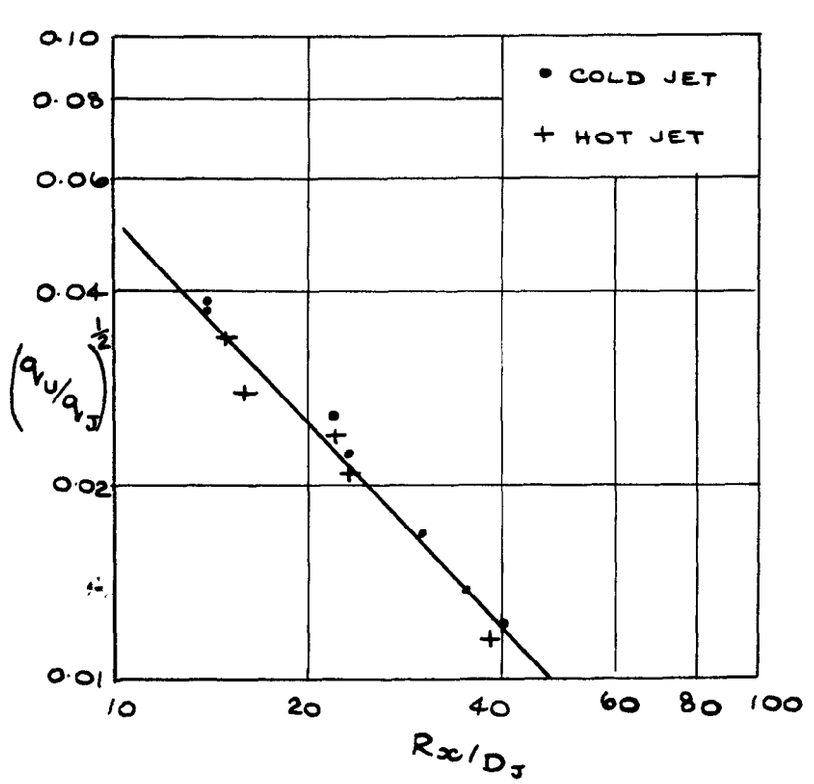

15b

EFFECT OF U/V_J AND θ_J ON FORWARD EXTENT OF JETS FROM TAXIING SINGLE VERTICAL NOZZLE

FIG.16.

a) MOVING NOZZLE

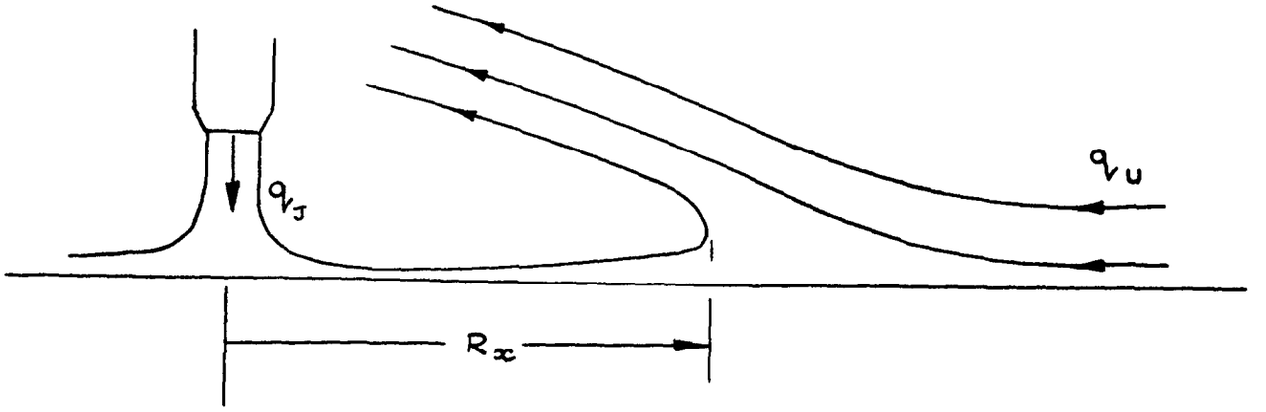

b) STATIONARY NOZZLE

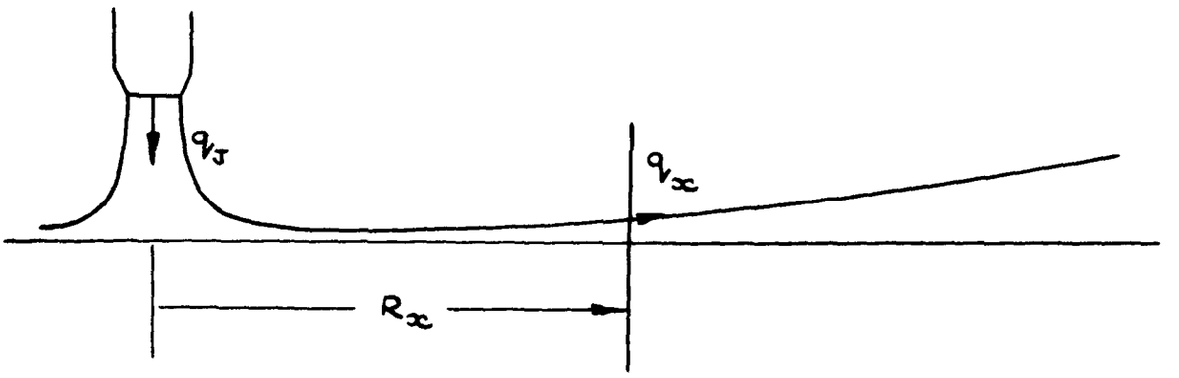

HORIZONTAL EXTENT OF JETS

FIG.17.

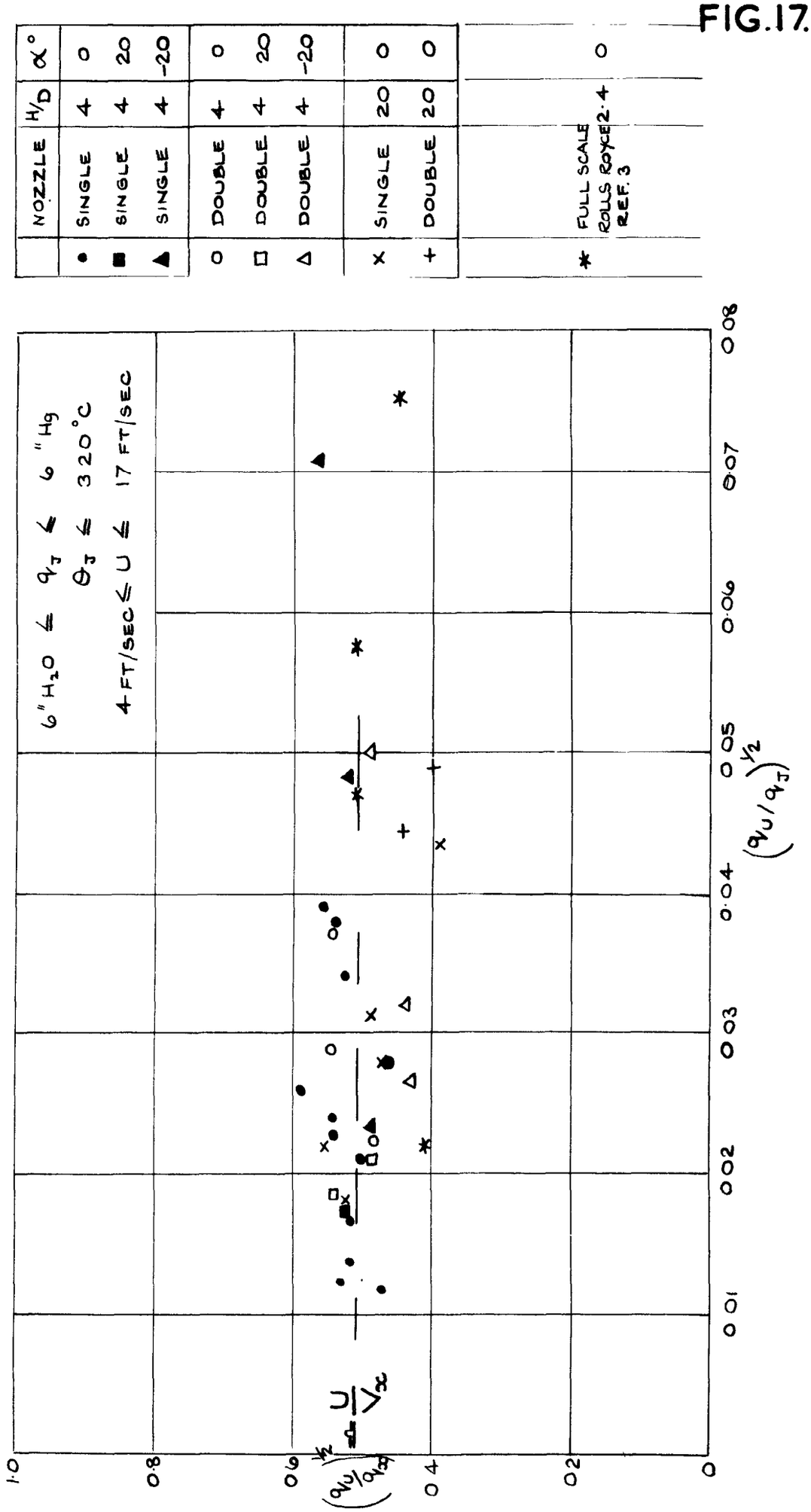

CORRELATION OF TAXI ING TESTS ON SINGLE AND DOUBLE NOZZLES

FIG. 18.

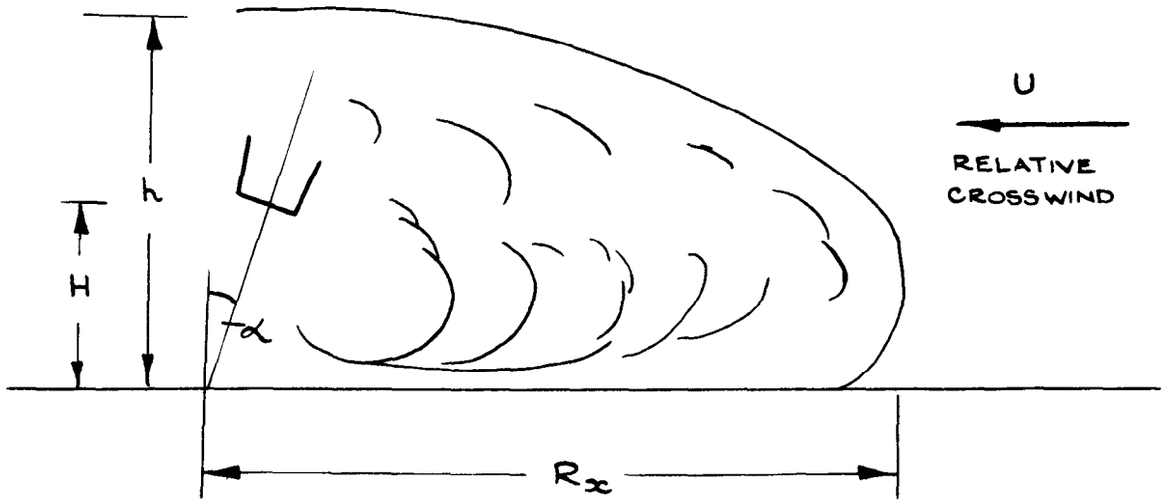

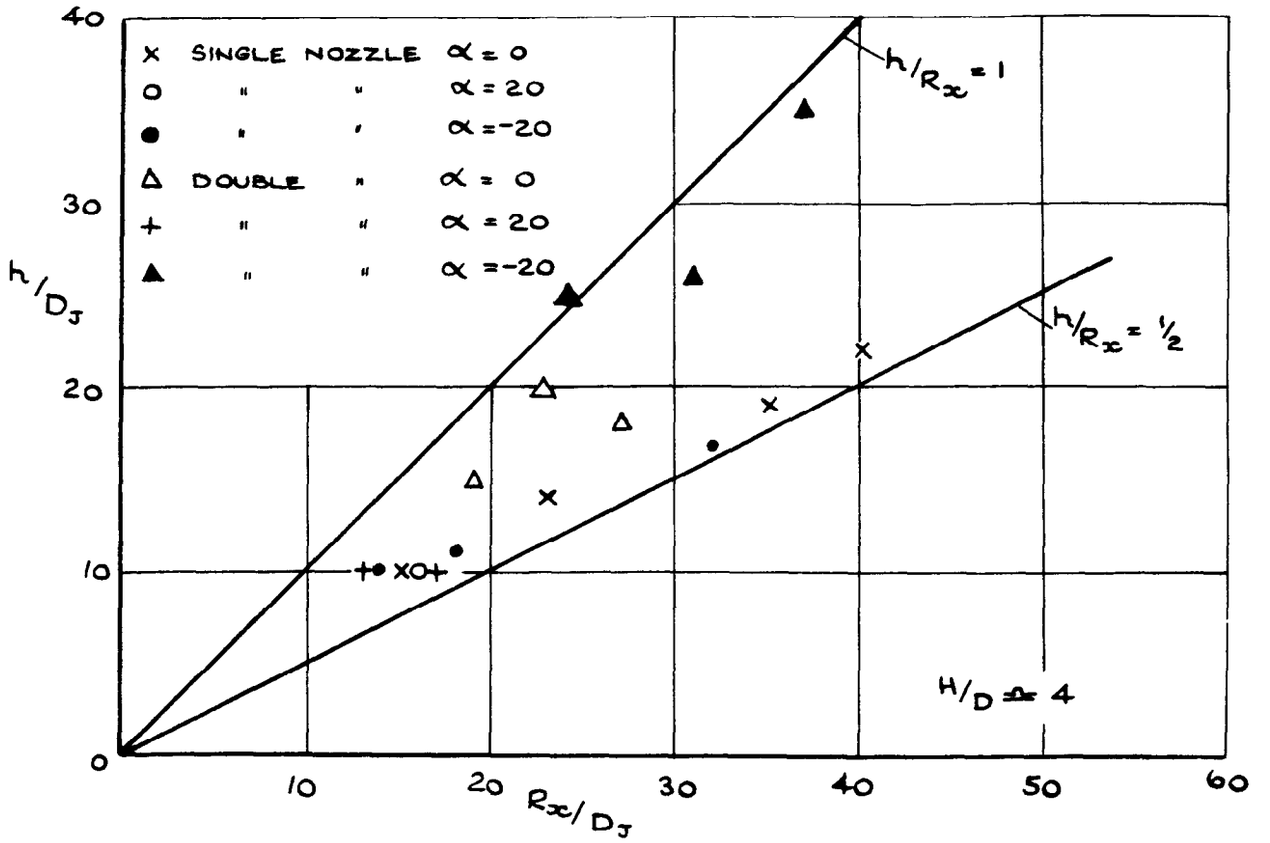

HEIGHT OF EXHAUST CLOUD, TAXI ING NOZZLE(S)

FIG. 19.

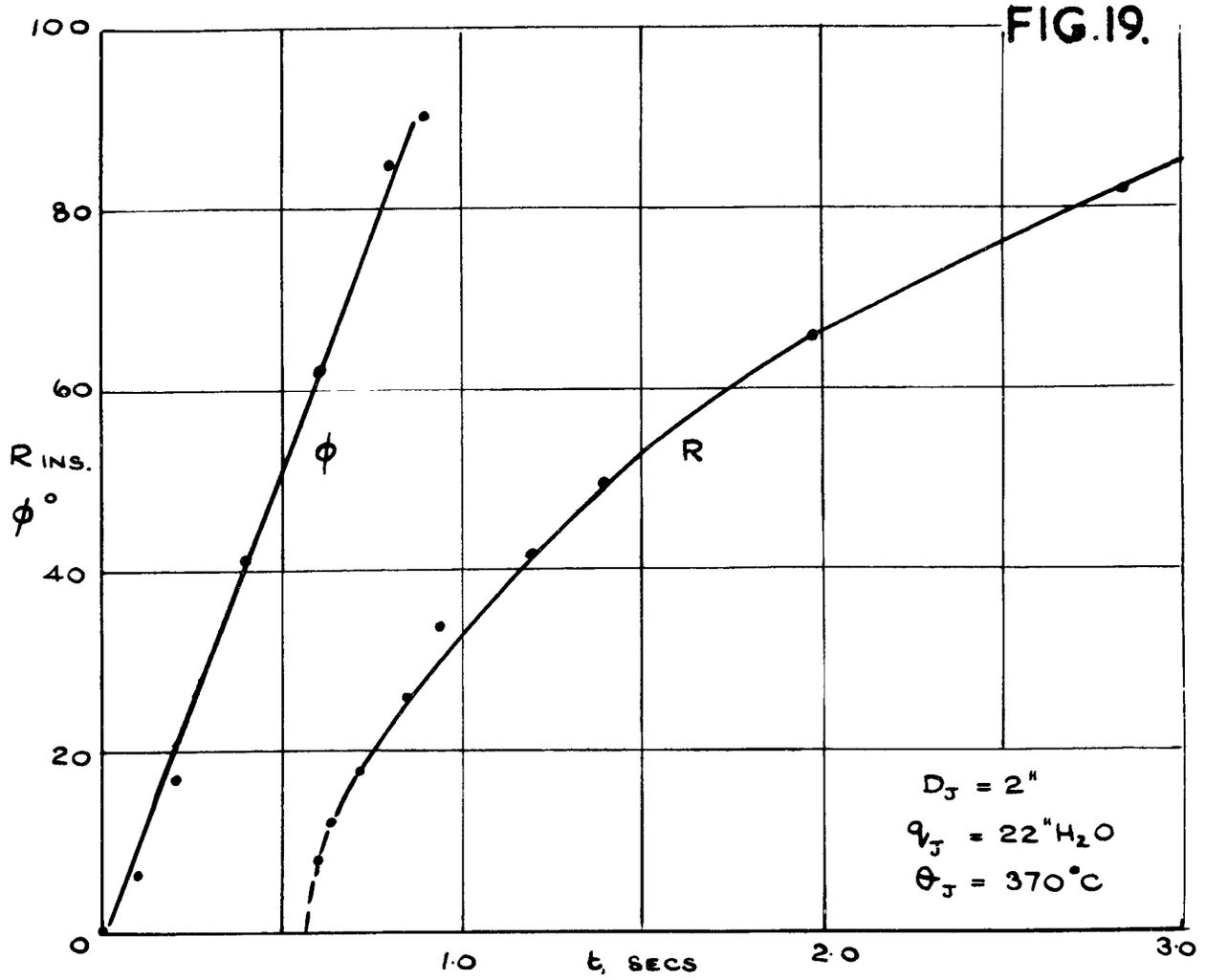

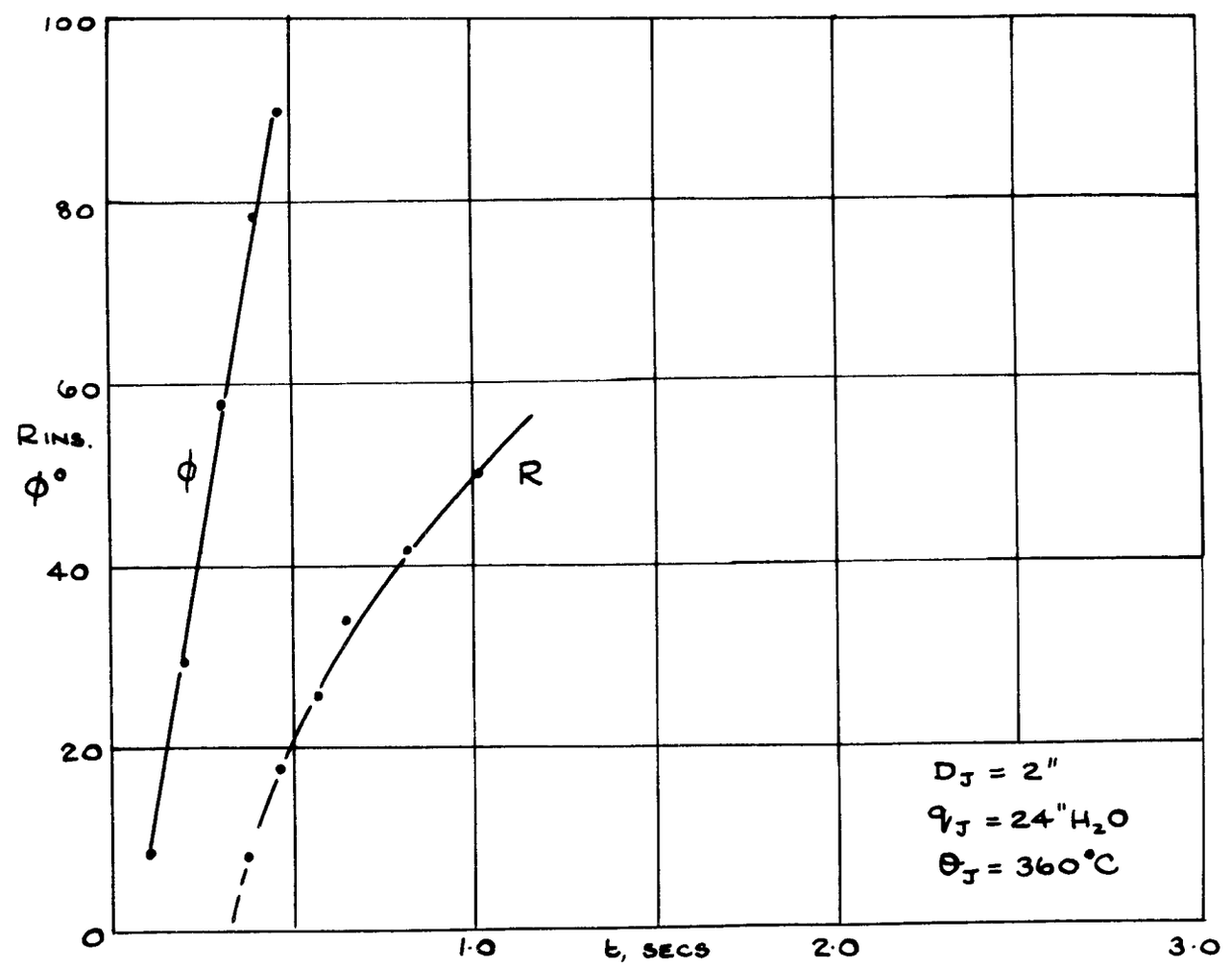

GROWTH OF JET ON SWIVELLING NOZZLE FROM HORIZONTAL TO VERTICAL. STATIC SINGLE NOZZLE

FIG.20.

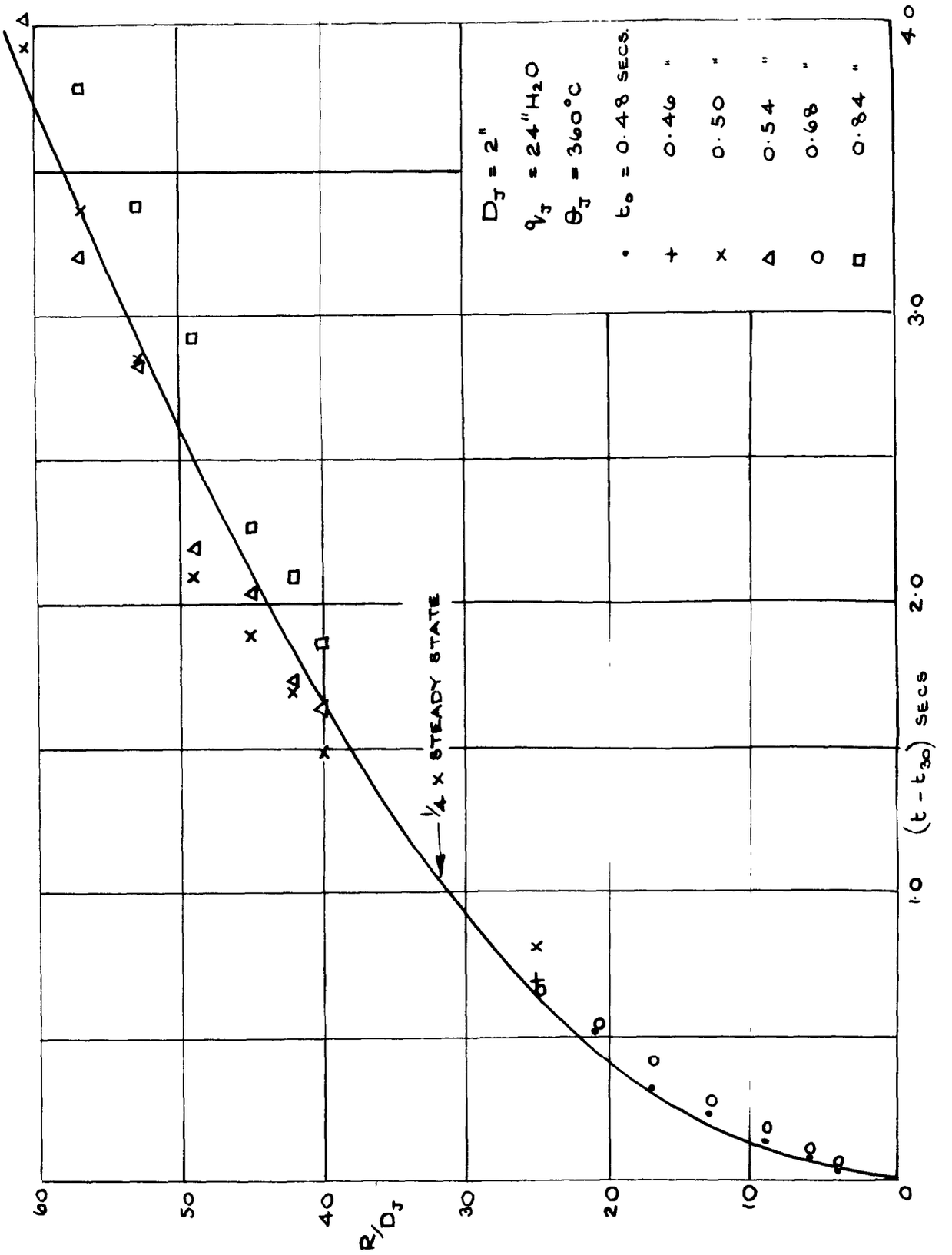

TRANSIENT GROWTH OF JET ON SWIVELLING NOZZLE SUDDENLY FROM HORIZONTAL TO VERTICAL

STATIC SINGLE NOZZLE

FIG.21.

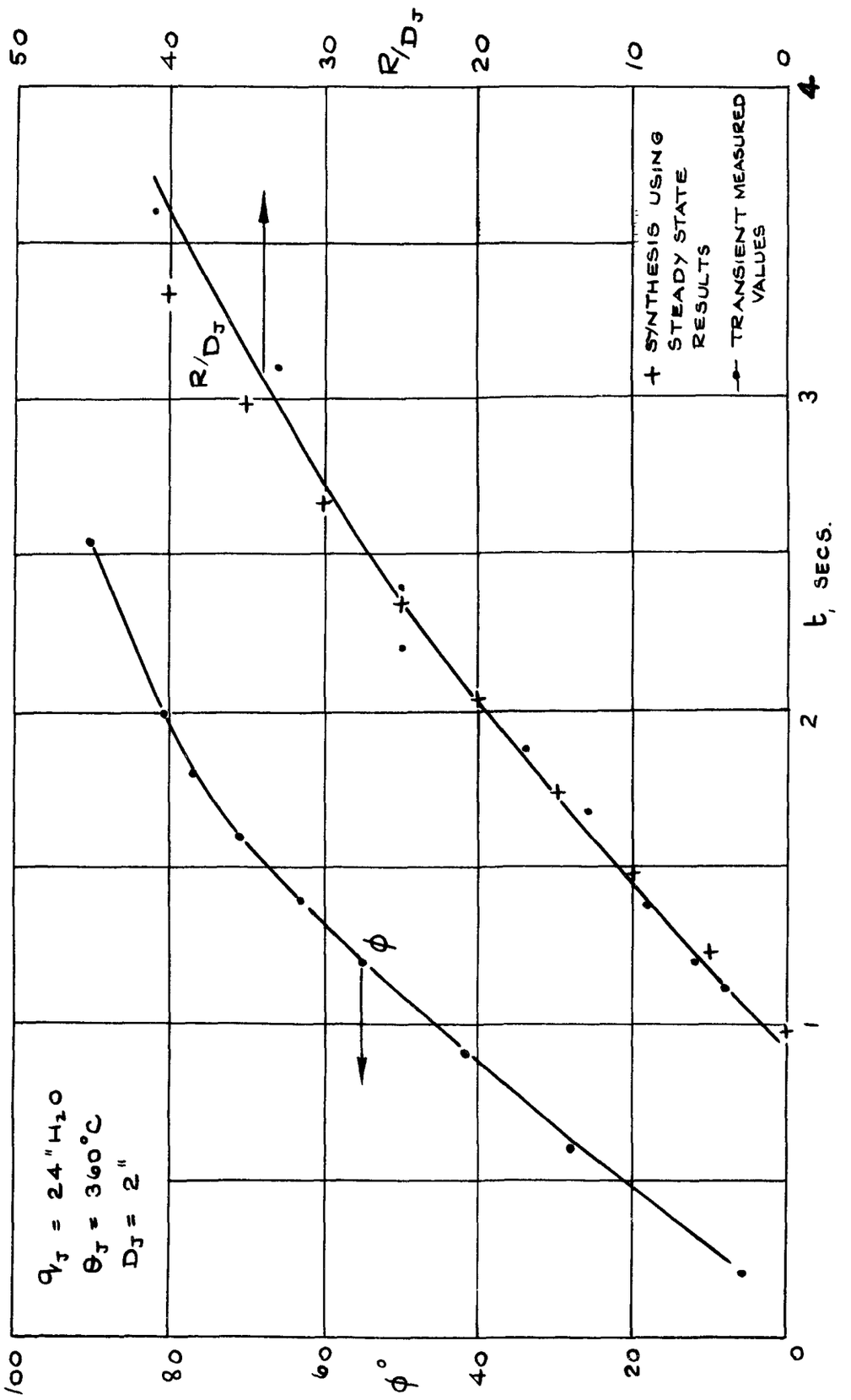

GROWTH OF JET ON SWIVELLING NOZZLE SLOWLY FROM HORIZONTAL TO VERTICAL

STATIC SINGLE NOZZLE

FIG.22.

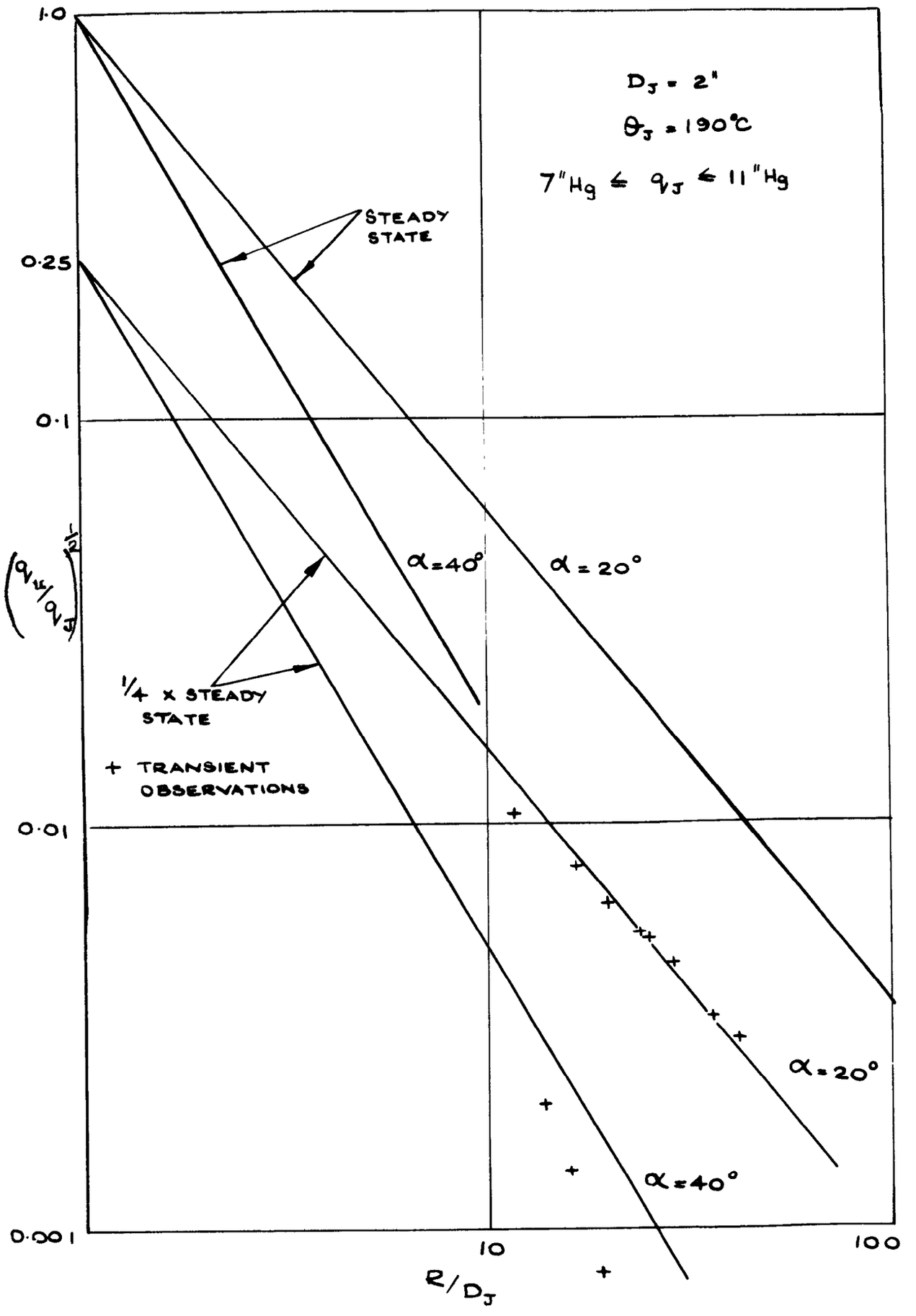

TRANSIENT VELOCITY OF JET ON SWIVELLING NOZZLE SUDDENLY FROM HORIZONTAL TO AN ANGLE α° TO THE VERTICAL STATIC SINGLE NOZZLE

FIG.23.

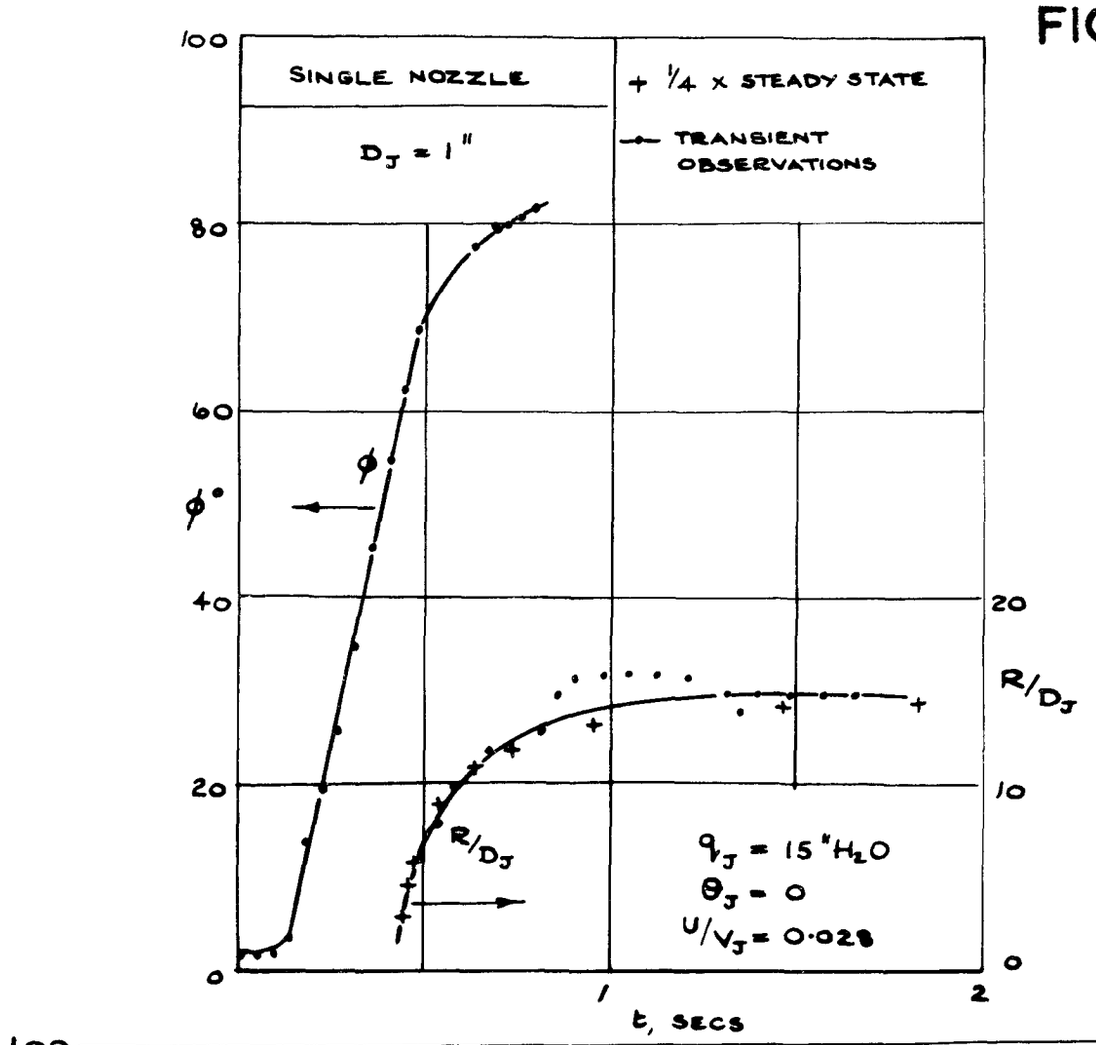

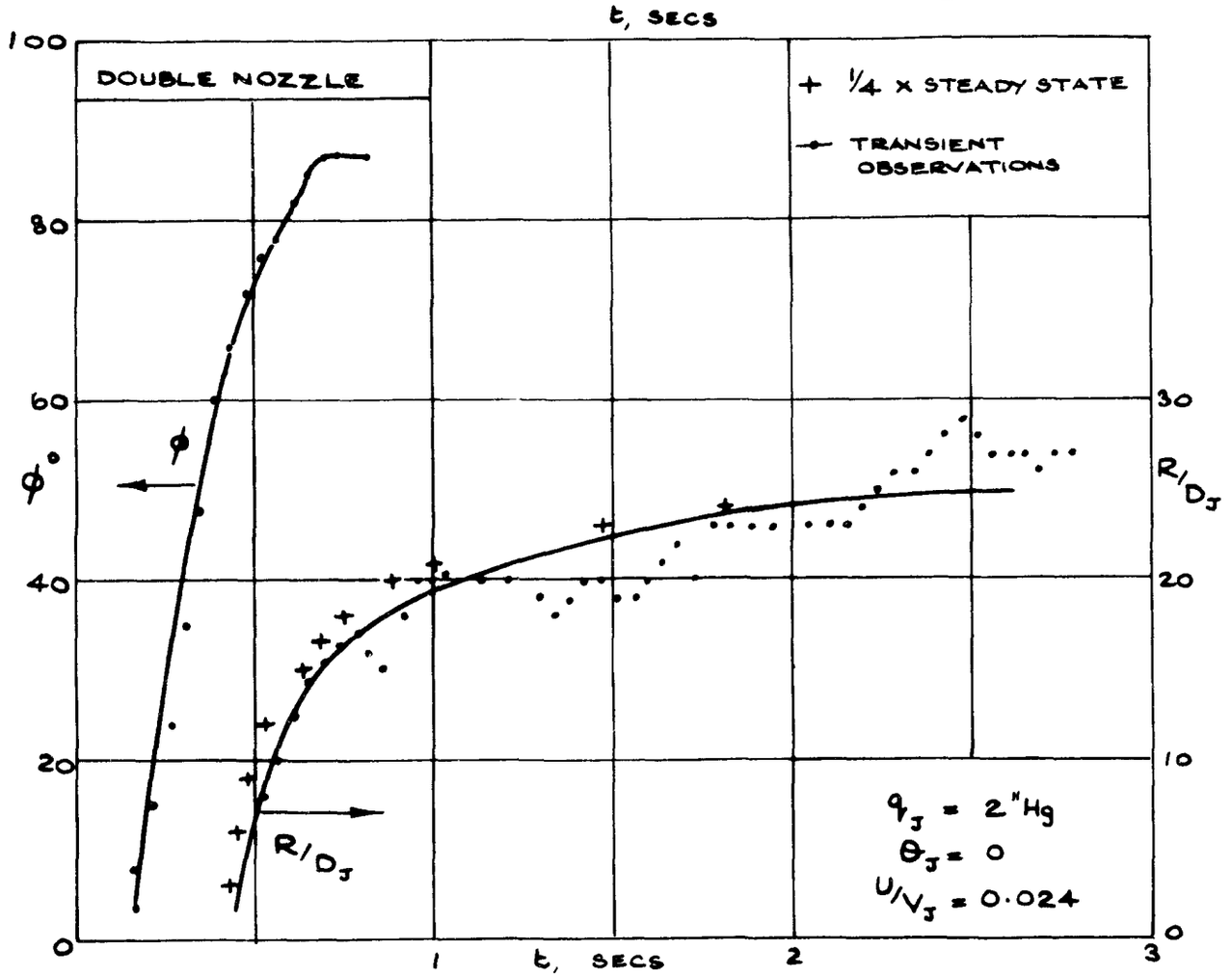

GROWTH OF JET ON SWIVELLING NOZZLES SUDDENLY FROM HORIZONTAL TO VERTICAL TAXIING SINGLE AND DOUBLE NOZZLES

FIG.24.

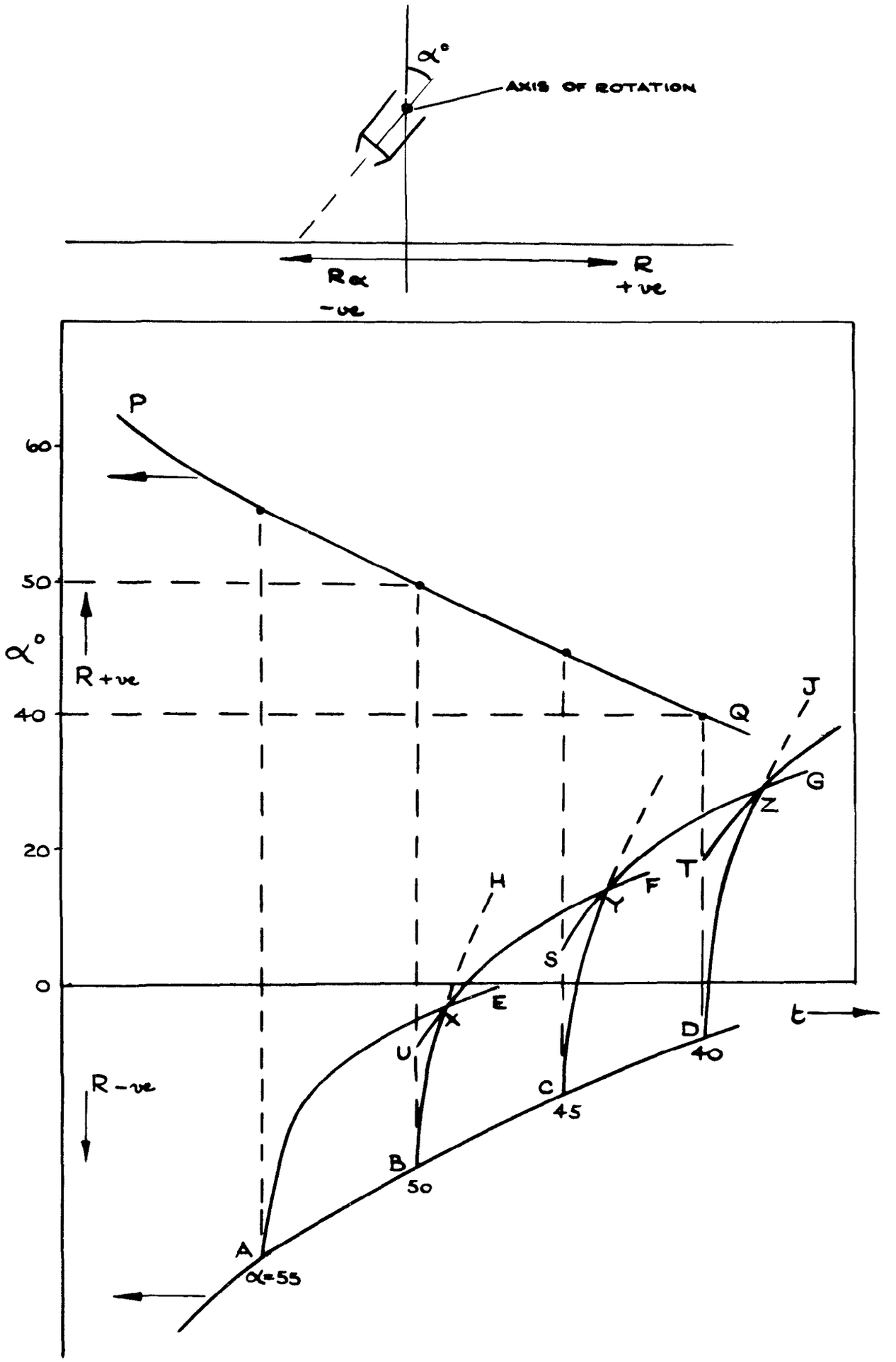

SYNTHESIS OF TRANSIENT GROWTH OF JET USING STEADY STATE VALUES FOR CASE WHEN NOZZLES ARE ROTATED SLOWLY TO VERTICAL

A.R.C. C.P. No. 911 532.525:533.691.18
October, 1964
Abbott, W. A.

STUDIES OF FLOW FIELDS CREATED BY VERTICAL AND INCLINED JETS WHEN STATIONARY OR MOVING OVER A HORIZONTAL SURFACE

Model tests have been carried out with single and twin nozzle arrangements, at varying inclinations. The decay of maximum velocity and temperature of the jet after impingement on the ground has been measured.

Transient effects associated with swivelling nozzles have been studied and measurements of the upwind extent and height of the exhaust cloud were made with the nozzles moving over the ground (taxiing). Empirical rules are given for estimating these effects from measurements made under static, steady-flow conditions.

A.R.C. C.P. No. 911 532.525:533.691.18
October, 1964
Abbott, W. A.

STUDIES OF FLOW FIELDS CREATED BY VERTICAL AND INCLINED JETS WHEN STATIONARY OR MOVING OVER A HORIZONTAL SURFACE

Model tests have been carried out with single and twin nozzle arrangements, at varying inclinations. The decay of maximum velocity and temperature of the jet after impingement on the ground has been measured.

Transient effects associated with swivelling nozzles have been studied and measurements of the upwind extent and height of the exhaust cloud were made with the nozzles moving over the ground (taxiing). Empirical rules are given for estimating these effects from measurements made under static, steady-flow conditions.

A.R.C. C.P. No. 911 532.525:533.691.18
October, 1964
Abbott, W. A.

STUDIES OF FLOW FIELDS CREATED BY VERTICAL AND INCLINED JETS WHEN STATIONARY OR MOVING OVER A HORIZONTAL SURFACE

Model tests have been carried out with single and twin nozzle arrangements, at varying inclinations. The decay of maximum velocity and temperature of the jet after impingement on the ground has been measured.

Transient effects associated with swivelling nozzles have been studied and measurements of the upwind extent and height of the exhaust cloud were made with the nozzles moving over the ground (taxiing). Empirical rules are given for estimating these effects from measurements made under static, steady-flow conditions.

A.R.C. C.P. No. 911 532.525:533.691.18
October, 1964
Abbott, W. A.

STUDIES OF FLOW FIELDS CREATED BY VERTICAL AND INCLINED JETS WHEN STATIONARY OR MOVING OVER A HORIZONTAL SURFACE

Model tests have been carried out with single and twin nozzle arrangements, at varying inclinations. The decay of maximum velocity and temperature of the jet after impingement on the ground has been measured.

Transient effects associated with swivelling nozzles have been studied and measurements of the upwind extent and height of the exhaust cloud were made with the nozzles moving over the ground (taxiing). Empirical rules are given for estimating these effects from measurements made under static, steady-flow conditions.

DETACHABLE ABSTRACT CARDS

Printed and published by

HER MAJESTY'S STATIONERY OFFICE

To be purchased from
49 High Holborn, London W.C.1
423 Oxford Street, London W.1
13A Castle Street, Edinburgh 2
109 St. Mary Street, Cardiff
Brazennose Street, Manchester 2
50 Fairfax Street, Bristol 1
35 Smallbrook, Ringway, Birmingham 5
80 Chichester Street, Belfast 1
or through any bookseller

Printed in England

C.P. No. 911

S.O. Code No. 23-9017-11